

**ISTANBUL TECHNICAL UNIVERSITY ★ INFORMATICS INSTITUTE**

**COMPUTATIONAL STUDY ON THE SIDE REACTIONS OF DOPA  
DECARBOXYLASE**

**M.Sc. THESIS**

**Erdem ÇİÇEK**

**Department of Computational Science and Engineering**

**Computational Science and Engineering Programme**

**JUNE 2013**



**ISTANBUL TECHNICAL UNIVERSITY ★ INFORMATICS INSTITUTE**

**COMPUTATIONAL STUDY ON THE SIDE REACTIONS OF DOPA  
DECARBOXYLASE**

**M.Sc. THESIS**

**Erdem ÇİÇEK  
(702091020)**

**Department of Computational Science and Engineering**

**Computational Science and Engineering Programme**

**Thesis Advisor: Doç. Dr. F. Aylin SUNGUR**

**JUNE 2013**



**İSTANBUL TEKNİK ÜNİVERSİTESİ ★ BİLİŞİM ENSTİTÜSÜ**

**DOPA DEKARBOKSİLAZ ENZİMİNİN YAN REAKSİYONLARI ÜZERİNE  
HESAPSAL BİR ÇALIŞMA**

**YÜKSEK LİSANS TEZİ**

**Erdem ÇİÇEK  
(702091020)**

**Hesaplamalı Bilim ve Mühendislik Anabilim Dalı**

**Hesaplamalı Bilim ve Mühendislik Programı**

**Tez Danışmanı: Doç. Dr. F. Aylin SUNGUR**

**HAZİRAN 2013**



**Erdem ÇİÇEK**, a **M.Sc.** student of ITU, **Informatics Institute 702091020**, successfully defended the thesis entitled **COMPUTATIONAL STUDY ON THE SIDE REACTIONS OF DOPA DECARBOXYLASE**”, which he prepared after fulfilling the requirements specified in the associated legislations, before the jury whose signatures are below.

**Thesis Advisor :**     **Doç. Dr. F. Aylin SUNGUR**     .....  
İstanbul Technical University

**Jury Members :**     **Doç. Dr. Adem TEKİN**     .....  
İstanbul Technical University

**Doç. Dr. Nurcan TÜZÜN**     .....  
İstanbul Technical University

**Date of Submission : 3 February 2014**  
**Date of Defense : 4 June 2013**





## **FOREWORD**

I would like to express my special appreciation and thanks to my advisor Assist. Professor Dr. F. Aylin SUNGUR, you have been a tremendous mentor for me. I would like to thank you for encouraging my research and for allowing me to grow as a research scientist. Your advice on both research as well as on my career have been priceless. I would also like to thank my jury members, I also want to thank you for letting my defense be an enjoyable moment, and for your brilliant comments and suggestions, thanks to you. I would especially like to thank staff in the Graduate School of Science Engineering and Technology at Istanbul Technical University. All of you have been there to support me when I recruited patients and collected data for my MSc. thesis.

A special thanks to my family. Words cannot express how grateful I am to my mother, father and my sisters for all of the sacrifices that you have made on my behalf. Your prayer for me was what sustained me thus far. I would also like to thank all of my friends who supported me in writing, and incited me to strive towards my goal.

June 2013

Erdem ÇİÇEK



## TABLE OF CONTENTS

	<u>Page</u>
<b>FOREWORD</b> .....	vii
<b>TABLE OF CONTENTS</b> .....	ix
<b>ABBREVIATIONS</b> .....	xi
<b>LIST OF FIGURES</b> .....	xv
<b>1. INTRODUCTION</b> .....	<b>1</b>
<b>2. METHODOLOGY</b> .....	<b>9</b>
2.1 The Schrödinger Equation .....	9
2.2 The Born Oppenheimer Approximation.....	12
2.3 The Hartree-Fock Equations .....	13
2.4 Slater-type Orbitals (STOs) and Gaussian-type Orbitals (GTOs) .....	14
2.5 Semi-Empirical Methods .....	16
2.5.1 Zero Differential Overlap (ZDO) approximation .....	17
2.5.2 PM3 .....	18
2.6 Density Functional Theory (DFT).....	18
2.6.1 Hybrid functionals.....	21
2.6.2 Basis Set.....	22
2.7 Solvation Effect.....	23
2.7.1 Polarized continuum models.....	24
2.8 Population Analysis.....	26
2.8.1 Natural Bond Order (NBO) analysis.....	26
2.9 Potential Energy Surface (PES) and Conformational Analysis.....	27
2.10 Computational Details .....	28
<b>3. RESULTS AND DISCUSSION</b> .....	<b>31</b>
3.1 Model Structures .....	32
3.2 Conformational Analysis .....	33
3.3 D-tryptophan Methyl ester.....	36
3.3.1 External aldimine formation .....	36
3.3.2 Quinonoid formation .....	39
3.3.3 Ketimine formation .....	39
3.4 5-Hydroxy Tryptophan (Serotonin) .....	43
3.4.1 External aldimine formation .....	43
3.4.2 Quinonoid formation .....	45
3.4.3 Ketimine formation .....	47
3.5 Solvent Effect.....	49
<b>4. CONCLUSION</b> .....	<b>55</b>
<b>REFERENCES</b> .....	<b>57</b>
<b>APPENDICES</b> .....	<b>63</b>
<b>CIRRICULUM VITAE</b> .....	<b>67</b>



## ABBREVIATIONS

$\text{\AA}$	: Angstrom
$\psi$	: Wave function
$\hbar$	: Planck's constant
$V$	: Potential energy
$G$	: Gibbs free energy
$m$	: Mass
$\nabla^2$	: Laplacian
$Z$	: Atomic number
$\epsilon_0$	: Permittivity constant
$r$	: Distance
$H_{\text{tot}}$	: Total Hamiltonian
$T_n$	: Kinetic energy of nuclei
$T_e$	: Kinetic energy of electrons
$V_{\text{nc}}$	: Potential energy of nuclear – electron attraction
$V_{\text{ee}}$	: Potential energy of electron – electron repulsion
$H_e$	: Electronic Hamiltonian operator
$E_e$	: Electronic energy
$H_n$	: Nuclear Hamiltonian operator
$\epsilon_i$	: One electron energy eigenvalues
$\chi_i$	: Spin orbital
$H^{\text{core}}$	: Core Hamiltonian
$\zeta$	: Coulomb operator
$\xi$	: Exchange operator
$f_i$	: Fock operator
$N$	: Quantum number
$L$	: Quantum number
$m_l$	: Quantum number
$N$	: Normalization constant
$Y_{lm_l}$	: Spherical harmonic
$n_{\text{eff}}$	: Effective principal quantum number
$Z_{\text{eff}}$	: Effective atomic number
$\phi$	: Atomic orbital
$P_{tu}$	: Density matrix elements
$H_{rs}^{\text{core}}$	: Core integral
$F_{rs}$	: Fock matrix element
$S$	: Unit matrix
$E_j$	: Coulomb repulsion between electrons
$E_{\text{XC}}$	: Exchange – correlation energy
$E_{\text{X}}$	: Exchange energy
$E_{\text{C}}$	: Correlation energy

$\epsilon_X$	: Exchange energy per particle
$\epsilon_c$	: Correlation energy per particle
$E_X^{Becke}$	: Becke's exchange functional
$\lambda$	: Coupling parameter
$U_{XC}^\lambda$	: Exchange – correlation energy according to coupling parameter
$u_{xc}$	: Exchange correlation potential density
$E_{XC}^{LSDA}$	: Exchange correlation energy from LSDA
$E_{XC}^{B3LYP}$	: Exchange correlation energy from B3LYP
$E^{HF}$	: Hartree – Fock energy
$E_C^{VWN}$	: Vosko, Wilk, Nusair function
$E_C^{LYP}$	: LYP correlation functional
$\phi_s$	: Basis function
$c_{si}$	: Coefficient of $s^{th}$ basis function according to $i^{th}$ MO
$d_{si}$	: Coefficient of primitive Gaussian function
$E_{EN}$	: Distortion energy
$G_{ENP}$	: Electrostatic component of solvation
$G_{cavity}$	: Thermal free energy in cavity
$G_{dispersion}$	: Thermal free energy of dispersion
$G_{electrostatic}$	: Electrostatic thermal free energy
$q$	: Charge
$\epsilon$	: Dielectric constant
$\gamma_k$	: Reduced density matrix of order k
<b>R</b>	: Gas constant
<b>T</b>	: Temperature
<b>K</b>	: Boltzman function
<b>kcal</b>	: Kilocalory
<b>PLP</b>	: Pyridoxal 5 – phosphate
<b>PMP</b>	: Pyridoxamine 5 – phosphate
<b>5-HT</b>	: Serotonin,
<b>D-TrpMe</b>	: D-Tryptophan Methyl Ester
<b>DDC</b>	: Dopa Decaroxylase
<b>PHE</b>	: Phenylalanine
<b>ARG</b>	: Arginine
<b>ILE</b>	: Isoleucine
<b>GLU</b>	: Glutamate
<b>THR</b>	: Threonine
<b>HF</b>	: Hartree – Fock
<b>STO</b>	: Slater – type orbital
<b>GTO</b>	: Gaussian – type orbital
<b>AO</b>	: Atomic orbital
<b>MO</b>	: Molecular orbital
<b>SCF</b>	: Self consistent field
<b>ZDO</b>	: Zero differential overlap
<b>PM3</b>	: Parametrized Model 3
<b>NDDO</b>	: Neglect of diatomic differential overlap
<b>AM1</b>	: Austin Model 1
<b>DFT</b>	: Density functional theory
<b>LDA</b>	: Local density approximation

<b>LSDA</b>	: Local spin density approximation
<b>B3LYP</b>	: Becke three-parameter Lee – Yang – Parr
<b>KS</b>	: Kohn – Sham
<b>PES</b>	: Potential energy surface
<b>PCM</b>	: Polarized continuum model
<b>NBO</b>	: Natural bond orbital
<b>NAO</b>	: Natural atomic orbital
<b>BO</b>	: Born Oppenheimer
<b>IEFPCM</b>	: Integral Equation Formalism PCM
<b>UFF</b>	: Universal Force Field
<b>SCRFF</b>	: Self Consistent Reaction Field
<b>G09</b>	: Gaussian 09
<b>IRC</b>	: Intrinsic reaction coordinate
<b>TS</b>	: Transition state





## LIST OF FIGURES

	<u>Page</u>
<b>Figure 1.1</b> : a) Crystal structure of DOPA Decarboxylase (PDB 1JS6 X Ray) b) Ribbon view of DOPA decarboxylase in complex with cofactor (PLP) and inhibitor (carbiDOPA) (PDB 1JS3 X Ray).....	3
<b>Figure 1.2</b> : Active site of DDC that involves the amino acids; Thr246, Lys303, His192 and PLP molecule. ....	4
<b>Figure 1.3</b> : Model compound and substrates used in calculations a) Model structure of DOPA Decarboxylase-PLP complex b) D-Tryptophan Methylester c) 5-HT, serotonin.....	7
<b>Figure 2.1</b> : Approximating of several Gaussian-type orbitals with a Slater-type orbital [43]. ....	16
<b>Figure 2.2</b> : A two dimensional gas-phase PES and the PES that derived from addition of solvation. Thick lines show a chemical reaction [43]. ....	24
<b>Figure 3.1</b> : Schematic representation of half transamination mechanisms of DDC with D-tryptophan methyl ester. a) Reaction path of PLP-5 - D-tryptophan methyl ester complex.....	31
<b>Figure 3.2</b> : Three dimensional geometries of model structures. a) Methylamine as Lys303. b) PLP-methylamine complex as PLP-Lys303 complex...	33
<b>Figure 3.3</b> : Three dimensional geometries of optimized (B3LYP/6-31+G(d,p)) geometries of 4 <sup>+</sup> -N-protonated internal aldimine. a) The lowest energy conformer. b) The second lowest energy conformer. ....	34
<b>Figure 3.4</b> : Three dimensional geometries of optimized (B3LYP/6-31+G(d,p)) geometries of D-tryptophan methylester and 5-HT conformers a) The lowest energy conformer of D-tryptophan methylester. b) The second lowest energy conformer of D-tryptophan methylester. C) The lowest energy conformer of 5-HT.....	35
<b>Figure 3.5</b> : Three dimensional geometries of formation of D-tryptophan methylester complex (structure 2). a) Structure 1a-1b Complex before transition state formation. b) Geometry optimization result from forward IRC calculation. c) Transition state (TS12) of PLP D-tryptophan methylester complex.....	37
<b>Figure 3.6</b> : a) Transition state (TS23) of PLP D-tryptophan methylester model complex. b) Geometry optimization result from forward IRC calculation. (Structure 3, 4 <sup>+</sup> -N-protonated external aldimine) .....	38
<b>Figure 3.7</b> : Three dimensional geometries of formation of quinonoid (structure 4). a) Transition state (TS34) with water assistance. b) Transition state (TS34) with Threonine assistance. c) Geometry optimization result from forward IRC calculation. (structure 4, quinonoid).....	40
<b>Figure 3.8</b> : Three dimensional geometries of formation of ketimine (structure 5). a) Transition state (TS45) with water assistance. b) Geometry	

optimization result from forward IRC calculation. (structure 5, ketimine). .....	41
<b>Figure 3.9</b> : Energy profile for D-TrpME - DDC mechanism in gas phase. Relative free energies are given as kcal/mol.....	42
<b>Figure 3.10</b> : Three dimensional geometries of formation of 5-HT complex (structure 2_s). a) Structure 1a_-1b_s Complex before transition state formation. b) Geometry optimization result from forward IRC calculation. ....	44
<b>Figure 3.11</b> : a) Transition state (TS23_s) of PLP 5-HT complex. b) Geometry optimization result from forward IRC calculation. (structure 3_s, 4'-N-protonated external aldimine).....	46
<b>Figure 3.12</b> : Three dimensional geometries of formation of quinonoid (structure 4_s). a) Transition state (TS34_s) with water assistance. b) Geometry optimization result from forward IRC calculation. (structure 4_s, quinonoid) .....	47
<b>Figure 3.13</b> : Three dimensional geometries of formation of ketimine (structure 5_s). a) Transition state (TS45_s) with water assistance.....	48
<b>Figure 3.14</b> : Energy profile for 5-HT - DDC mechanism in gas phase. Relative free energies are given as kcal/mol.....	50
<b>Figure 3.15</b> : Energy profile for D-TrpME - DDC mechanism in solvent phase. Relative free energies are given as kcal/mol.....	52
<b>Figure 3.16</b> : Energy profile for 5-HT- DDC mechanism in solvent phase. Relative free energies are given as kcal/mol.....	53

## COMPUTATIONAL STUDY ON THE SIDE REACTIONS OF DOPA DECARBOXYLASE

### SUMMARY

Main catalytic activity of the pyridoxal 5-phosphate dependent Dopa Decarboxylase (DDC) is the conversion of the aromatic amino acids into the corresponding aromatic amines via decarboxylation reaction. Transamination reaction occurs as a side reaction, which decreases the activity of the enzyme. The reactions of Dopa decarboxylase (DDC) with d-enantiomers of tryptophan methyl ester was studied experimentally where a quinonoid intermediate detected for the first time [1]. The experimental results also indicated that the 5-hydroxytryptamine (5-HT, serotonin) acts both as a substrate and as a mechanism based inactivator of DDC for low pH cases. The corresponding aldehyde and ammonia molecules formed following the transamination reaction [2]. The computational studies mostly focused on the decarboxylation reaction of DDC.

There are no computational studies in literature based on the side reactions. In this study, transamination mechanism in the presence of two different substrates, namely, 5-HT (serotonin) and D-tryptophan methyl ester (D-TrpMe), were investigated using computational methods (B3LYP/6-31+G\*\*). Calculations at the B3LYP/6-31++G\*\* level were carried out in water, utilizing the integral equation formalism-polarizable continuum (IEF-PCM) model.

A DFT study is carried out on the side reactions of DDC which lowers the activity of the enzyme. The half-transamination reaction is one of the side reactions of DDC studied computationally in the presence of two different substrates. The structural differences between D-Trptophan Methyl Ester and 5-Hydroxytryptophan result in competitive inactivation mechanism.

The results enable us to have an idea about one of the side reactions of DDC. However, there exists another side reaction which can contain a radical in the pathway. For a better explanation of the competitive reactions, one must also study that pathway. It should be also noted that a QM/MM study will be carried out for this reaction in order to identify the specificity of amino acid residues surrounding the active site.



## DOPA DEKARBOKSİLİZ ENZİMİNİN YAN REAKSİYONLARI ÜZERİNE HESAPSAL BİR ÇALIŞMA

### ÖZET

Özelleşmiş proteinler olan enzimler, kalıcı yapısal değişimlere uğramadan kimyasal reaksiyonların hızını artırıcı katalizör moleküllerdir [3]. Katalizleme, geçiş yapısı enerjilerinin düşürülmesi veya başlangıç yapısı enerjilerinin yükseltilmesi ile sağlanır [4]. Katalizlenen reaksiyon süresince reaktant ve ürünler arasındaki serbest enjji farkı ( $\Delta G$ ) değişmez [5].

Belirli enzimler, kimyasal reaksiyonlardaki katalizör fonksiyonunu yerine getirmek için koenzim isimli organik moleküllere ihtiyaç duyarlar. Koenzim molekülü enzimin aktif bölgesine bağlanarak kataliz reaksiyonunda doğrudan etki eder [4,6]. Kofaktör olarak adlandırılan inorganik yapılar olan  $Fe^{2+}$ ,  $Zn^{2+}$  gibi iyonlarda bazı enzimlerin katalizör fonksiyonu için gereklidir [6].

Vitamin B6'nın aktif formu olan PLP, ilgili enzimin  $\epsilon$ -amino grup lizin molekülü ile imin yapısını oluşturan organik kofaktördür [8, 9]. PLP protein olmamasına rağmen bir çok enzimde kofaktör molekül olarak bulunur. PLP ve enzim arasında oluşan yapı Schiff bazı oluşumu olarak da adlandırılır [10] ve bu yapı ilgili enzime göre çeşitli reaksiyonların katalizinde etkin bir role sahiptir [8]. PLP'nin en önemli fonksiyonlarından biri transaminasyon reaksiyonlarında koenzim olarak kullanılmasıdır. Bu sebeple PLP-bağımlı enzimlere ve gerçekleştirdikleri dekarboksilasyon,  $\beta$ -eliminasyon, aldol ayrılması, transaminasyon ve transiminasyon gibi çeşitli reaksiyonlara özel bir ilgi duyulur [8,11,12].

PLP-Schiff bazı oluşumuna yönelik yapılan hesapsal çalışmalar gösteriyorki PLP molekülü enzimin lizin amino asidine kovalent imin bağı ile bağlanarak içsel aldimin yapısını oluşturmaktadır [8,13,14]. Ayrıca substrat ile Schiff bazının reaksiyonu ile yeni bir imin bağı oluşur ve Michaelis kompleksi üzerinden dışsal aldimin yapısı meydana gelir [13,14,15]. Bu reaksiyon transaminasyon veya transaldiminzasyon olarak adlandırılır [11]. Bu çalışmalar neticesinde ortaya çıkan bir diğer sonuca göre bir çok PLP bağımlı enzimde yer alan piridin halkasındaki nitrojen atomu protonlanarak enzimatik yapıların stabilizasyonunu elektron-sink etkileşimi ile sağlamaktadır [14,15,16].

Aromatik amino asit dekarboksilaz (DDC, AADC, EC 4.1.1.28) enzimi PLP-bağımlı enzimler sınıfında yer almaktadır. PLP molekülü enzimin tüm alt birimlerinde yer almakla birlikte, Lys-303 amino asidine kovalent Schiff bazı ile bağlıdır. DDC enzimi homodimer yapıda olup her biri 480 amino asitten oluşur ve tahmini 54kDa moleküler ağırlığa sahiptir [17]. Enzim ile ilgili yapılan kristal yapı çalışmalarında elde edilen verilere göre her bir monomer 3 yapıdan meydana gelmektedir; bir  $\beta$ -sheet ve sekiz  $\alpha$ -heliks'ten oluşan büyük merkezi yapı, bir  $\beta$ -sheet ve üç  $\alpha$ -heliks'ten oluşan c-terminal küçük yapı ve iki  $\alpha$ -heliks'ten oluşan N-terminal yapı [18]. PLP molekülü alt birimlerin büyük merkezi yapılarında yer alır [19]. X-ray analizlerinin

ortaya çıkardığı bir diğer sonuca göre karboskil grup PLP halka yapısına dikey olarak konumlanmak zorundadır [21]. Histidin192, Aspartat271, Asparajin300 ve Histidin301 amino asitlerinin dışsal aldimin yapısı ile hidrojen bağları oluşturduğu tahmin edilmektedir. [18,22]. Bu amino asitlere yönelik yapılan nokta mutasyon çalışmaları sonucunda, enzimin dekarboksilasyon ve buna bağlı transaminasyon aktivitesinde ciddi düşüşler gözlemlenmiştir [22]. Enzimin her bir monomerinde, 328 ve 339 amino asitleri arasında esnek bir düğüm yapısı yer almaktadır [18]. *In vitro* çalışmalara göre bu esnek yapı proteolitik parçalanmadan sorumludur. PLP ve substratın varlığında enzim yapısında meydana gelen konformasyonel değişikliklerden ötürü proteolitik parçalanma engellenir [23]. Bu esnek yapının parçalanması da enzimin dekarboksilasyon aktivitesinde düşüslere yol açar [23].

Dopamin ve Serotonin DDC enzimin dekarboksilasyon reaksiyonu ile açığa çıkan aromatic aminlerdir. L-5-hidroksitriptofan (5-HTP)'ın katalizlenmesi ile dopamin elde edilirken, L-3,4-dihidroksifenilalanin (L-dopa)'ın katalizlenmesi ile serotonin yapısı elde edilir. Her iki molekülde sinir sisteminde, hücreler arası sinyal iletiminde önemli role sahiptir. Ayrıca bu moleküllerin işlevsel ve davranışsal süreçlerde çok çeşitli karmaşık fonksiyonları bulunmaktadır [3].

DDC enziminin eksikliği çeşitli klinik semptomlara yol açan dopamin ve serotonin yokluğuna yol açar [34]. Zihinsel yavaşlama, hipokinezi, okülogirik krizler, trunkal hipotoni, sarkma, sinirlilik, hipersalivasyon, vücut sıcaklığında dengesizlik ve aşırı terleme gibi klinik semptomlar DDC enziminin eksikliğinde ortaya çıkmaktadır [35]. Okülogirik krizler sebepleri tam olarak anlaşılamamış olsa bile, dopamin eksikliğinin hastalığa yol açtığı düşünülmektedir [36]. Uyku problemleri, vücut sıcaklığı dengesizliği ve ruh hali ile ilgili düzensizlikler ise serotonin eksikliği ile ilişkilendirilmiş semptomlardır [35].

Dopa Dekarboksilaz (DDC) enzimi piridoksal 5-fosfat (PLP) bağımlı enzim sınıfında olup ana mekanizması olan dekarboksilasyon reaksiyonu ile aromatik amino asitleri ilgili aromatik aminlere katalizler. Enzimin yan reaksiyonu olarak enzim aktivitesini düşüren transaminasyon reaksiyonu da gerçekleşir. Bu çalışmanın bir bölümünde de kullanılan triptofan metilesterin d-enantiyomeri (D-TrpMe) ile yapılan deneysel çalışma sonucunda ara molekül olarak ilk defa bir kuinonoid yapısı gözlemlenmiştir. [1]. Diğer deneysel sonuçlara göre yine bu çalışmada kullanılan 5-hidroksi triptofan (5-HT) substratı, düşük pH ortamında enzim için inaktivator olarak da davranmaktadır. İlgili inaktivasyon mekanizması süresince aldehid ve amonyum yapılarının oluştuğu da gözlemlenmiştir [2].

DDC enzimi ile ilgili yapılan hesapsal çalışmaların çoğunlukla enzimin ana reaksiyonu olan dekarboksilasyon mekanizması üzerine yoğunlaştığı söylenebilir. Literatürde enzimin yan reaksiyonları için gerçekleştirilen bir hesapsal çalışma bulunmamaktadır.

Bu çalışma kapsamında, enzimin farklı iki substratı olan serotonin (5-HT) ve d-triptofan metilester ile tranamination mekanizması hesapsal olarak aydınlatılmaya çalışılmıştır. Deneysel olarak öne sürülmüş olunan mekanizmalarda yer alan sabit yapılar B3LYP/6-31+G(d,p) teori seviyesinde optimize edilmiştir. Ayrıca çözücü etkisi de göz önüne alınmıştır.

Bu çalışma sonucunda elde edilen bilgiler ışığında, DDC enziminin gerçekleştirdiği transaminasyon reaksiyonunun mekanizması açıklanmaya çalışılmıştır. Ayrıca, yapılar arasındaki farklılıkların mekanizma üzerine etkileri de bu çalışma kapsamında elde edilen sonuçlardandır. Yan reaksiyonlar ile daha detaylı sonuçlar

için QM/MM çalışmalarının sürdürülmesi ve bu sayede aktif bölgede yer alan amino asit yapılarının etkisinin ortaya çıkarılması önerilmektedir.





## 1. INTRODUCTION

Enzymes are specialized proteins that are catalysts and increase the speed of a chemical reaction without themselves undergoing any permanent chemical change [3]. The catalysis provided by reducing the transition state energies and by increasing the ground state energies [4]. On the other hand, the free energy difference ( $\Delta G$ ) between the reactants and products does not change during the enzymatic reactions [5].

An active site is the part of an enzyme that directly binds to a substrate and carries a reaction [5]. Structure of active site and its chemical characteristic are of specific for the binding of a particular substrate [5].

The binding of the substrate to the enzyme causes changes in the chemical bonds of the substrate and causes the reactions that lead to the formation of products. The products are released from the enzyme surface to regenerate the enzyme for another reaction cycle. [5]. Therefore the first step in an enzyme catalyzed reaction is always the formation of the enzyme-substrate complex [3, 4]. Complementary shapes between enzyme and substrate(s) allow a greater amount of weak non-covalent interactions including electrostatic forces, Van der Waals forces, hydrogen bonding, and hydrophobic interactions [4].

In an active site, there are two important regions for catalytic power, one of them binds the substrate (substrate binding region) while the other catalyzes the reaction (catalytic region). In some enzymes the substrate binding region involves the catalytic region [5].

Coenzymes are organic molecules that are required by certain enzymes to carry out catalysis. They bind to the active site of the enzyme and participate in catalysis but are not considered substrates of the reaction. [4, 6]. A cofactor could be either an inorganic ion such as  $Fe^{2+}$ ,  $Zn^{2+}$ , or an organic complex which is specifically called coenzyme [6, 7]. Some enzymes may need both a coenzyme and an inorganic ion [6].

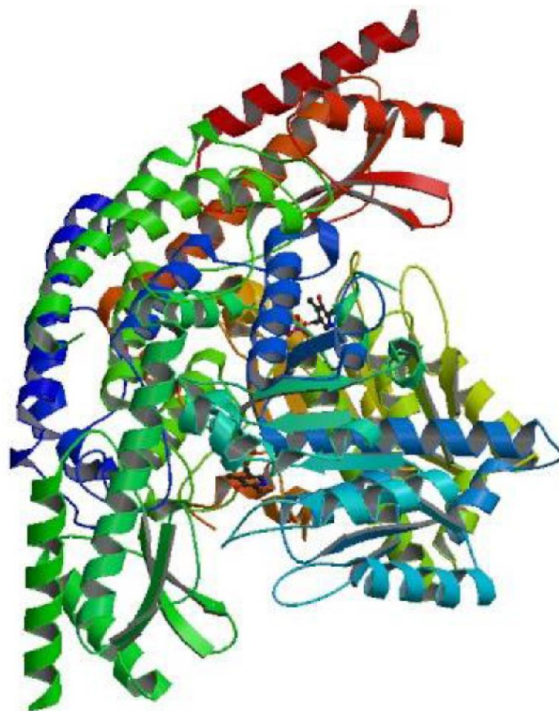
Coenzymes are a kind of transition carriers that are usually derived from vitamins [6, 7].

PLP, is the active form of vitamin B6 [8], which is an organic cofactor in which it forms an imine with  $\epsilon$ -amino group of a lysine residue of PLP-dependent enzymes [9]. PLP is not a protein, but acts as a co-factor for a number of enzymes and protein groups. Furthermore the formation of imine could be referred as Schiff base formation [10] which takes place in lots of different chemical reactions that leads different products based on the enzyme [8]. One of the main functions of pyridoxal phosphate is as a coenzyme in transamination reactions. Thus, there is a particular interest about the PLP-dependent enzymes due to the diversity of chemical reactions such as decarboxylation,  $\beta$ -elimination, aldol cleavage, transamination and transamination [8, 11, 12].

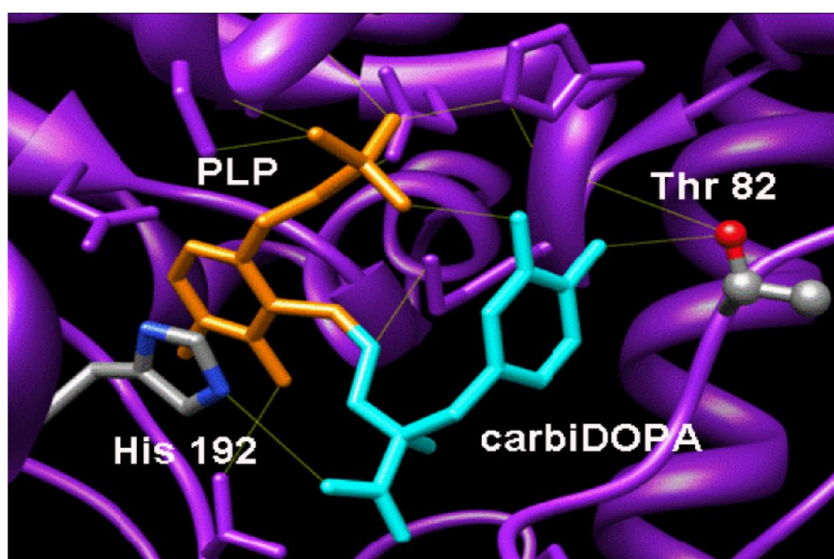
According to the computational studies that concentrate on the formation of PLP-Schiff base [13, 14], an internal aldimine structure is formed when PLP is bound to lysine residue with an imine bond and bound to the enzyme covalently [8, 13]. Moreover, a new imine bond is formed due to the reaction of the substrate with the Schiff base that produces external aldimine from Michaelis complex [13, 14, 15]. This reaction is called transamination or transaldimination which is symmetrical [11]. It is also known that [14, 15] in most PLP dependent enzymes the nitrogen of pyridine ring is protonated and this protonation stabilizes the interactions in enzymatic residues [16]. This stabilization is achieved due to the electron-sink effect [14, 16].

Aromatic amino acid decarboxylase () (DDC, EC 4.1.1.28), a member of subfamily II of  $\alpha$ -family of pyridoxal 5-phosphate (PLP) dependent enzymes, in which all subunits contains an active site PLP that is covalently bound to Lys-303 via a Schiff base. DDC is a homodimeric enzyme consisting of two 480 amino acid monomers each with a predicted molecular weight of 54kDa [17]. According to the analysis of crystal structure, each monomer consists of three domains; a large central domain of one  $\beta$ -sheet and eight  $\alpha$ -helices; a c-terminal small domain of one  $\beta$ -sheet and three  $\alpha$ -helices; and an N-terminal domain containing two  $\alpha$ -helices (Figure 1.1) [18]. The homodimer binds two molecules of PLP, one molecule within the large domain of each monomer [19]. The x-ray analysis results pointed out that the carboxyl group must lie perpendicular to the plane of the PLP ring [21]. It is predicted that the

residues Histidine192, Aspartate271, Asparagine300 and Histidine302 are all form hydrogen bonds with the external aldimine [18, 22]. Studies based on the mutations of each of these residues revealed that a great reduction has occurred in decarboxylation activity and decarboxylation dependent transamination activity [22].



(a)



(b)

**Figure 1.1 :** a) Crystal structure of DOPA Decarboxylase (PDB 1JS6 X Ray) b) Ribbon view of DOPA decarboxylase in complex with cofactor (PLP) and inhibitor (carbiDOPA) (PDB 1JS3 X Ray).

There is a flexible loop region between amino acids 328 and 339 in each monomer [18]. According to in vitro results; this region is responsible for the proteolytic cleavage. In the presence of PLP and substrate the cleavage is prevented because of the conformational changes in the structure [23]. Also cleavage of this flexible region causes reduced decarboxylase activity [23].

The active site of DDC (Figure 1.2) is located close to the monomer-monomer interface and is composed of residues mostly of one monomer but with residues Isoleucine101 and Phenylalanine103 contributed from the opposing monomer [18]. The active site contains Lysine303, forms an internal aldimine with PLP through a Schiff base linkage. This PLP-lysine linkage undergoes a transaldimination reaction with the substrate forming a Schiff base between PLP and the substrate, the external aldimine, leaving the amino group of the lysine residue as a free base. Site directed mutagenesis of Lysine303 demonstrates that this residue has further roles in the catalytic mechanism of DDC including involvement in the hydrolysis reaction that separates PLP from the decarboxylation product [20].

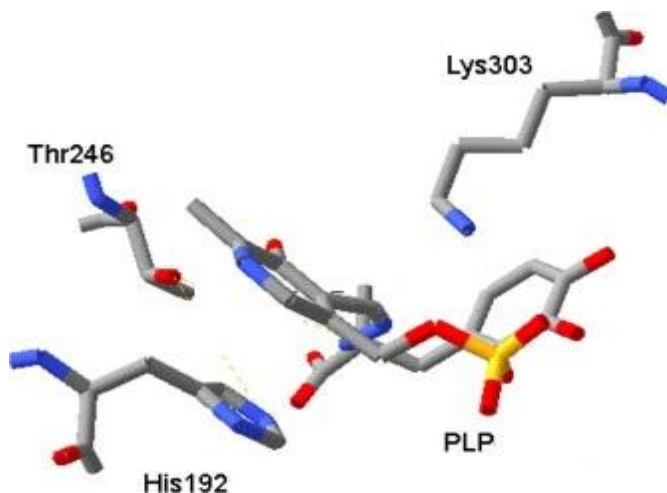


**Figure 1.2 :** Active site of DDC that involves the amino acids; Thr246, Lys303, His192 and PLP molecule.

Dopamine and Serotonin are aromatic amines derived from the decarboxylation of the amino acids L-5-hydroxytryptophan (5-HTP) and L-3,4-dihydroxyphenylalanine (L-dopa) respectively, by the enzyme aromatic L-amino acid decarboxylase (AADC; EC No. 4.1.1.28). These two molecules have important extracellular molecular signaling role within the nervous system and in peripheral tissues. Both serotonin and dopamine have been demonstrated to play a complex role in a range of physiological and behavioral processes [3].

Serotonin has been demonstrated to participate in a wide range of behavioral functions [24]. Serotonin is also considered to be important for the maintenance of sleep such that deficiency of serotonin has been shown to disturb sleep or some stages of sleep [25]. Eating behavior is also thought to be modulated by serotonin. Serotonin reuptake inhibitors and non-selective serotonin agonists have been found to reduce food intake and induce satiety. According to findings are suggestive of an organic hyperphagia and weight gain related to the serotonin deficiency [26, 27]. Moreover serotonin is known to play a complex role in the control of mood and emotion, for example serotonin depletion enhances cognitive and behavioral responses to fearful stimuli [28, 29]. Further roles of serotonin include modulation of body temperature, movement and memory [30].

The dopamine dependent pathways in the brain are considered to be involved in a range of behavioral and cognitive functions. It is known that the dopamine pathway plays an essential role in the planning and execution of voluntary movement that are controlled by basal-ganglia motor circuits [31]. Dopamine is also considered to be involved in working and learning memory [32]. Furthermore dopamine is found to modulate motivational behavior, which can be disrupted with dopamine antagonists [33].

Absence of serotonin and dopamine can be caused by a deficiency of AADC, which catalysis conversion of 5-HTP to serotonin and L-dopa to dopamine [34]. The majority of clinical symptoms include mental retardation, hypokinesia, oculogyric crises, truncal hypotonia, ptosis, irritability, hypersalivation, temperature instability and excessive sweating are also shared with AADC deficiency [35]. The etiology of oculogyric crises is not well understood, however as they have not been reported in dopamine  $\beta$ -hydroxylase deficiency this could suggest that they are specifically related to dopamine deficiency [36]. Examples of symptoms likely to involve serotonin deficiency include sleeping difficulties, temperature instability and problems with mood [35].

Main catalytic activity of the pyridoxal 5-phosphate dependent Dopa Decarboxylase (DDC) is the conversion of the aromatic amino acids into the corresponding aromatic amines via decarboxylation reaction. DOPA decarboxylase (DDC) is responsible for the synthesis of the key neurotransmitters dopamine and serotonin via decarboxylation of L-3,4-dihydroxyphenylalanine (L-DOPA) and L-5-

hydroxytryptophan (5-HTP), respectively. DDC takes place in side reactions like oxidative deamination and transamination reactions in addition to its major role in the decarboxylation [37, 38].

DDC takes place in side reactions like oxidative deamination and transamination reactions in addition to its major role in the decarboxylation. In anaerobic medium, conditions a deamination reaction occurs subsequent to decarboxylation producing 3,4-dihydroxyphenylacetaldehyde and pyridoxamine 5''-phosphate [37]. Superoxide anion and hydrogen peroxide were observed as the products of the oxidative deamination reactions [38]. In aerobic conditions in addition to the decarboxylation there is a possibility of the formation of Pictet-Spengler adducts between L-dopa or 5-HTP and PLP [37]. This reaction leads to the removal of the PLP coenzyme from the active site and consequently inactivates the protein.

Transamination reaction occurs as a side reaction during the decarboxylation mechanism. 5-hydroxytryptamine (5-HT) is one of the substrates in the decarboxylation reaction. However, experimental results indicate that the 5-HT acts both as a substrate and as a mechanism based inactivator of DDC in the transamination reaction. The corresponding aldehyde and ammonia molecules are formed following the transamination reaction [39]. The physiological characteristics of this side reaction are unknown however enhancement of side reactions has been demonstrated in several artificially generated AADC mutants [22].

In this thesis, a DFT study is carried out on the side reactions of DDC which lowers the activity of the enzyme. A model is used to represent an enzyme in addition to the PLP without a phosphate group and two different substrates namely, 5-HT and D-tryptophan methyl ester (Figure 1.3). The computational studies mostly focused on the formation of a Schiff base and the decarboxylation reaction of DDC. However, to our best knowledge, there are not any computational studies in literature based on the side reactions of the DDC in the presence of 5-HT and D-tryptophan methyl ester as a substrate. The results will be discussed in the light of the previous computational findings obtained by Konuklar et al. in addition to the experimental results found in the literature. The results will enable us to explain both the substrate effect and the solvent effect on the transamination reaction mechanism.

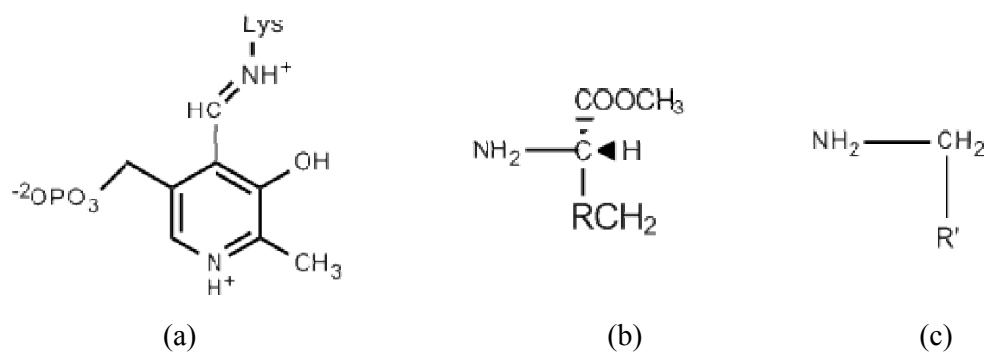


**Figure 1.3 :** Model compound and substrates used in calculations a) Model structure of DOPA Decarboxylase-PLP complex b) D-Tryptophan Methyl ester c) 5-HT, serotonin.





## 2. METHODOLOGY

### 2.1 The Schrödinger Equation

Erwin Schrödinger introduced a differential equation in 1926 where the wave function  $\Psi(r_1, r_2, \dots, t)$  evolves in time according to the equation

$$\hbar \frac{\partial \Psi(x,t)}{\partial t} = -\frac{\hbar^2}{2m} \frac{\partial^2 \Psi}{\partial x^2} + V(x)\Psi(x,t) \quad (2.1)$$

In this equation, which is called time dependent Schrödinger equation,  $\Psi$  is the wave function,  $\hbar$  is Planck's constant,  $m$  is mass of particle and  $V$  is the potential field. [41] The first step to solve the Schrödinger equation is expressing the wave function  $\Psi(x,t)$  as the product of two functions [42]

$$\Psi(x,t) = \psi(x)\chi(t) \quad (2.2)$$

Where the  $\psi(x)$  depends only the distance  $x$  and  $\chi(t)$  depends only the time  $t$ . If these function are substituted on the equation (2.1) and the partial derivatives are taken, it gives

$$i\hbar\psi(x)\frac{d\chi(t)}{dt} = -\frac{\hbar^2}{2m}\chi(t)\frac{d^2\psi(x)}{dx^2} + V(x)\psi(x)\chi(t) \quad (2.3)$$

If the both sides are divided by  $\psi(x)\chi(t)$  it gives

$$i\hbar \frac{1}{\chi(t)} \frac{d\chi(t)}{dt} = -\frac{\hbar^2}{2m} \frac{1}{\psi(x)} \frac{d^2\psi(x)}{dx^2} + V(x) \quad (2.4)$$

In equation (2.3) the left hand side depends only time while the right hand side depends only distance. Therefore when  $x$  changes only the right hand side changes. However the right hand side is equals to the left hand side, thus the right hand side of the equation (2.4) must equal to a constant value. Due to the dimension of a constant are those of energy, the separation constant is determined as  $E$ , which is assumed that it is a real number [41, 42]. In consequence the equation could be separated into two

parts, one time dependent and one spatial dependent. The time dependent part is shown by the equation

$$i\hbar \frac{d\chi(t)}{dt} = E\chi(t) \quad (2.5)$$

which has a solution of

$$\chi(t) = e^{-iEt/\hbar} \quad (2.6)$$

Therefore the substitution of equation (2.6) to the equation (2.2), the complete wave function has the form

$$\Psi(x,t) = e^{-iEt/\hbar} \psi(x) \quad (2.7)$$

The spatial dependent equation is given by

$$-\frac{\hbar^2}{2m} \frac{d^2\psi(x)}{dx^2} + V(x)\psi(x) = E\psi(x) \quad (2.8)$$

In this equation if the left hand side is written with the parenthesis in which whole part has the same multiplier  $\psi(x)$  it gives

$$\left[ -\frac{\hbar^2}{2m} \frac{d^2}{dx^2} + V(x) \right] \psi(x) = E \psi(x) \quad (2.9)$$

where the part in the parenthesis is referred as the Hamiltonian operator ( $\hat{H}$ ).

The Hamiltonian operator expresses the total energy in term of position and momentum [42].

$$\hat{H} = \left[ -\frac{\hbar^2}{2m} \frac{d^2}{dx^2} + V(x) \right] \quad (2.10)$$

Therefore, the time independent Schrödinger equation finally has the form of

$$\hat{H} \psi(x) = E \psi(x) \quad (2.11)$$

According to the equation (2.10) Hamiltonian is made up of both the kinetic energy and the potential energy

$$\hat{H} = T + V \quad (2.12)$$

where T is the kinetic energy operator which is related to linear momentum and V is the potential energy operator. In one dimension a particle with mass m has a kinetic energy as

$$T = -\frac{\hbar^2}{2m} \frac{d^2}{dx^2} \quad (2.13)$$

In three dimension the operator in the position representation is

$$T = -\frac{\hbar^2}{2m} \left\{ \frac{\partial^2}{\partial x^2} + \frac{\partial^2}{\partial y^2} + \frac{\partial^2}{\partial z^2} \right\} = -\frac{\hbar^2}{2m} \nabla^2 \quad (2.14)$$

where  $\nabla^2$  (del, squared) is called the Laplacian. For an n particle system kinetic energy will have the form of

$$T = -\frac{\hbar^2}{2m} \sum_{i=1}^n \nabla_i^2 \quad (2.15)$$

Potential energy term in Hamiltonian is the Coulomb potential energy of an electron in the field of a nucleus which has an atomic number of Z

$$V = -\frac{Ze^2}{4\pi\epsilon_0 r} \quad (2.16)$$

where  $\epsilon_0$  is the permittivity constant and r is the distance from the nucleus to electron.

Therefore the potential energy term would be given

$$V = \frac{1}{4\pi\epsilon_0} \left[ - \sum_i^{\text{electrons}} \sum_j^{\text{nuclei}} \left( \frac{Z_i e^2}{\Delta r_{ij}} \right) + \sum_i^{\text{electrons}} \sum_{j<i}^{\text{electrons}} \left( \frac{e^2}{\Delta r_{ij}} \right) + \sum_i^{\text{nuclei}} \sum_{j<i}^{\text{nuclei}} \left( \frac{Z_i Z_j e^2}{\Delta R_{ij}} \right) \right] \quad (2.17)$$

where the electron-nuclear attraction is represented with the first term, electron-electron repulsion is represented with the second term and the nuclear-nuclear repulsion is represented with the last term.

## 2.2 The Born Oppenheimer Approximation

Schrödinger equation can not be solved analytically due to the number of particles in systems, even there are three particles in the simplest molecule  $H_2^+$  [41]. Born-Oppenheimer approximation takes into account the great differences in masses of electrons and nuclei to overcome the difficulty of Schrödinger equations for many particle systems. Due to the great differences between the masses of electrons and nuclei, electrons respond to the displacements of nuclei immediately. For this reason taking the position of nuclei fixed could be useful to solve Schrödinger equation [41].

The nucleus is much slower than electrons due to the differences in masses. Therefore separation of Schrödinger equation into two parts could be a good approximation, which is called Born-Oppenheimer approximation. In separated form, one part describes the electronic wave function for a fixed nuclear geometry while the other part, where wave function plays the role of potential energy, describes the nuclear wave function. According to the approximation, the electronic wave function depends only on the nuclear position not their momenta.

The total Hamiltonian is then written as

$$H_{tot} = T_n + T_e + V_{nc} + V_{ee} + V_{nn} \quad (2.18)$$

where the kinetic energy of nuclei and electrons are represented as  $T_n$  and  $T_e$  respectively, and the potential energies of nuclear-electron attraction as  $V_{nc}$ , electron-electron repulsion as  $V_{ee}$  and nuclear-nuclear repulsion as  $V_{nn}$ . Thus, if the Hamiltonian operator is transformed to a centre of mass system it gives

$$H_{tot} = T_n + H_e \quad (2.19)$$

where  $H_e$  is the electronic Hamiltonian operator which depends only on the nuclear position and could be written as

$$H_e = T_{en} + V_{ne} + V_{ee} + V_{nn} \quad (2.20)$$

If this Hamiltonian is used in electronic Schrödinger equation

$$H_e \psi_e (R,r) = E_e(R)\psi_e(R, r) \quad (2.21)$$

$$H_n \psi_n (R) = E_{tot}\psi_n(R) \quad (2.22)$$

$$(T_n + E_e(R)) \psi_n (R) = E_{tot}\psi_n(R) \quad (2.23)$$

where R and n denote nuclear coordinates while r and e denote electronic coordinates.

The nuclear Hamiltonian  $H_n$ , describes the vibrational, rotational and translational states of nuclei. Moreover the solution of the equation (2.23) allows to lay out the molecular potential energy curve, and generally to construct potential energy surface of a polyatomic system [41].

### 2.3 The Hartree-Fock Equations

Hartree-Fock (HF) calculations are the simplest ab initio method. The problem that has been focused on is the infeasibility of the solution of Schrödinger equation for many particle systems [19].

The total wave function of an atom could be approximated as a combination of the wave function for different energy levels. Hartree's guess was depends on this fact and the method writes an approximate wave function for an atom as the product of one-electron wave function

$$\Psi_0 = \psi_0(1)\psi_0(2)\psi_0(3) \dots \psi_0(n) \quad (2.24)$$

The equation 2.24 is called the Hartree product where  $\Psi_0$  is a function of the coordinates of all electrons and  $\psi_0(1)$  is the function of coordinate of electron 1 and so on. The one electron wavefunctions are called atomic orbital if the dealed system is an ato [19]. In the case of a molecule  $\Psi_0$  is called molecular orbital. [19] The zeroth approximation to the total wavefunction is  $\Psi_0$ .

The eigenvalue of  $\Psi_0$  could be found by the equation

$$H\Psi_0 = H \psi_0(1)\psi_0(2)\psi_0(3) \dots \psi_0(n)$$

$$H\Psi_0 = \left( \sum_{i=1}^N \varepsilon_i \right) \Psi_0 \quad (2.25)$$

which proves the energy eigenvalue of a many-electron wave function is the sum of one-electron energy eigenvalue [21].

An electron on the spin orbital  $\chi_i$ , which is in the field of the nuclei and other electrons, has a Hamiltonian operator which contains three different contributions to the energy. Those contributions are the core Hamiltonian operator, Coulomb operator and the exchange operator [20]. Thus the Hamiltonian could be written as

$$H^{\text{core}}(1)\chi_i + \sum_{j \neq i}^N \zeta_j(1)\chi_i(1) - \sum_{j \neq i}^N \xi_j(1)\chi_i(1) = \sum_j \varepsilon_{ij}\chi_j(1) \quad (2.26)$$

where  $H^{\text{core}}(1)$  is the core Hamiltonian,  $\zeta_j(1)$  is Coulomb and  $\xi_j(1)$  exchange operators. If the equation is simplified according to the  $\{\zeta_i(1) - \xi_i(1)\}\chi_i(1) = 0$

$$f_i\chi_i = \sum_j \varepsilon_{ij}\chi_j \quad (2.27)$$

where  $f_i$  is called the Fock operator

$$f_i(1) = H^{\text{core}}(1) + \sum_{j=1}^N \{\zeta_i(1) - \xi_i(1)\} \quad (2.28)$$

while for a closed shell system it has the following form

$$f_i(1) = H^{\text{core}}(1) + \sum_{j=1}^{N/2} \{2\zeta_i(1) - \xi_i(1)\} \quad (2.29)$$

## 2.4 Slater-type Orbitals (STOs) and Gaussian-type Orbitals (GTOs)

The orbital of an atom of atomic number  $Z$  is written as

$$\phi_{nlm_l}(r, \theta, \phi) = N r^{n_{\text{eff}}-1} e^{-Z_{\text{eff}} \rho / n_{\text{eff}}} Y_{lm_l}(\theta, \phi) \quad (2.30)$$

Where  $n$ ,  $l$ ,  $m_l$  are the quantum numbers,  $N$  is the normalization constant,  $Y_{lm_l}$  is the spherical harmonic and  $\rho = r/a_0$ .  $n_{\text{eff}}$  is the effective principal quantum number which is related to the true principal quantum number  $n$  by the following map [41].

$$n \rightarrow n_{\text{eff}}: 1 \rightarrow 1 \quad 2 \rightarrow 2 \quad 3 \rightarrow 3 \quad 4 \rightarrow 3.7 \quad 5 \rightarrow 4.0 \quad 6 \rightarrow 4.2 \quad (2.31)$$

Orbitals with different values of quantum number  $n$  but same values of quantum numbers  $l$  and  $m_l$  are not orthonormal to each other. Moreover, s-orbitals with  $n > 1$  have zero amplitude at the nucleus in the case of Slater-type orbitals (STOs) [41].

Slater-type orbitals are mathematical functions to define the wave function of an electron in an atom, however they are not suitable for many electron atoms. [43] They are generally used in atomic or diatomic system calculations if high accuracy is required and also in semiempirical methods in which three and four centre integrals are not taken into account [44].

Although STOs have a number of attractive features, in ab initio HF theory they are limited. If the basis functions are chosen as STOs, there would be no analytical solution for the four index integral [21]. In 1950 Boys suggested an alternative to the usage of STOs that uses  $e^{-r^2}$  instead of  $e^{-r}$  where the AO-like functions have the form of a Gaussian function [45]. This AO-like functions are called Gaussian type orbitals (GTO) which are mathematical functions to define the wave function [48, 49].

The normalized GTO in atom-centered Cartesian coordinate is

$$\phi(x, y, z; \alpha, i, j, k) = \left(\frac{2\alpha}{\pi}\right)^{3/4} \left[\frac{(8\alpha)^{i+j+k} i! j! k!}{(2i)! (2j)! (2k)!}\right]^2 x^i y^j z^k e^{-\alpha(x^2+y^2+z^2)} \quad (2.32)$$

where  $\alpha$  is the exponent that controls the width of GTO and  $i, j, k$  are non-negative integers that order the nature of the orbital in a Cartesian sense. GTO has a spherical symmetry when all of these integers are zero and it is referred as s-type GTO. If one of the indices is equal to one the function is called p-type GTO where it has an axial symmetry about a single axis. Moreover, if the sum of the indices is equal to two, it is called d-type GTO [21].

On the other hand STO calculations require less primitives than GTO basis sets to define the wave function which is also seen in Figure 2.1 [43].

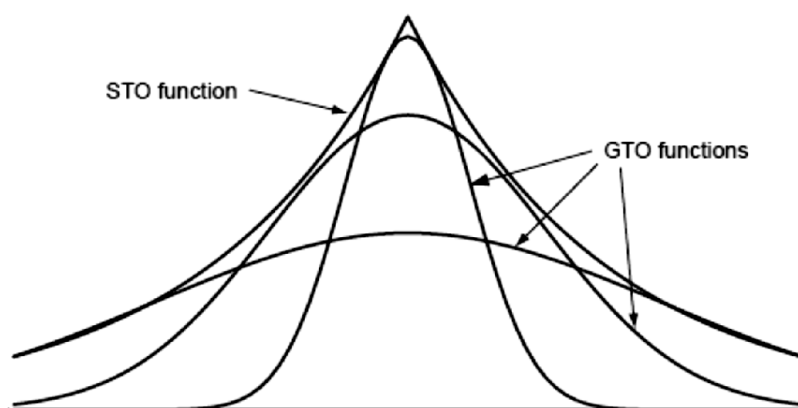


**Figure 2.1** : Approximating of several Gaussian-type orbitals with a Slater-type orbital [43].

The wave functions are defined by a finite number of functions by choosing a standard GTO basis set. Thus, the calculation approximates that an infinite number of GTO functions would be needed to define an exact wave function [43]. Although the real hydrogenic atomic orbitals have a cusp, GTOs are smooth and differentiable at the nucleus. Moreover, the GTOs is exponential in  $r^2$ , which results a rapid reduction in amplitude with distance for the GTOs, while the hydrogenic atomic orbitals are exponential in  $r$  [21].

## 2.5 Semi-Empirical Methods

In an ab initio calculation the core integral  $H_{rs}^{core}$ , density matrix elements  $P_{tu}$ , and the electronic repulsion integrals  $(rs/tu)$ ,  $(ru/ts)$  are used to calculate the Fock matrix element

$$F_{rs} = H_{rs}^{core}(1) + \sum_{t=1}^m \sum_{u=1}^m P_{tu} \left[ (rs|tu) - \frac{1}{2} (ru|ts) \right] \quad (2.33)$$

where density matrix is given as

$$P_{tu} = 2 \sum_{i=1}^{n/2} c_{ti} c_{ui} \quad (2.34)$$



and core integral is given as

$$H_{rs}^{\text{core}} = \int ds_1 \phi_r(1) \left[ -\frac{1}{2} \nabla^2 - \sum_{i=1}^k \frac{Z_i}{|r_1 - R_i|} \right] \phi_s(1) \quad (2.35)$$

An initial guess of the coefficients to calculate the density matrix values  $P_{tu}$  is necessary where it would be calculated by a simple Hückel calculation or extended Hückel calculation. To improve the energy levels and coefficients the Fock matrix of  $F_{rs}$  elements is diagonalized continually.

In an ab initio calculation much numbers of basis functions could be used. On the other hand semi-empiric methods use the basis functions which correspond to the atomic orbitals and Slater functions are used in SCF-type semi-empirical methods instead of the approximating them as sum of Gaussian functions. Moreover, semi-empirical calculations taken into account only the valence or the  $\pi$  electrons, thus the elements of core turn out an atomic nucleus plus its core electrons [19].

The cost of HF calculations is arise from the two-electron integrals which are necessary to construct the Fock matrix. Semi-empirical methods reduce the number of these integrals by taking them as zero to reduce the computational cost [44]. The integrals that are ignored are one-electron integrals involving three centers which are neglected by differential overlap [19, 44].

Furthermore, in SCF-type semi-empirical methods the overlap matrix is taken as a unit matrix ( $S=1$ ). Therefore the Roothaan-Hall equations  $FC = SCE$  are clear away without using orthogonalizing matrix to transform this equations into standard eigenvalue form  $FC = CE$  [19].

### 2.5.1 Zero Differential Overlap (ZDO) approximation

Zero Differential Overlap approximation is the center of semi-empirical methods. The approximation neglects all products of basis functions that depend of the same electron coordinates on different atoms [44]. The basis functions are taken to be orthonormal according to the equation (2.36) and the ZDO expands this idea to the two-electron integrals [46].

$$\int \chi_i(r) \chi_j(r) d\tau = \begin{cases} 1 & \text{if } i = j \\ 0 & \text{otherwise} \end{cases} \quad (2.36)$$

$$\frac{e^2}{4\pi\epsilon_0} \int \dots \frac{1}{r_{12}} \chi_i(r_1)\chi_j(r_1)d\tau_1 \quad (2.37)$$

If  $i$  and  $j$  equals to each other ( $i=j$ ) the integral is set to zero and the two-electron integrals have the form of

$$\frac{e^2}{4\pi\epsilon_0} \int \chi_i(r_1)\chi_j(r_1) \frac{1}{r_{12}} \chi_k(r_2)\chi_l(r_2)d\tau_1d\tau_2 \quad (2.38)$$

are set to zero unless  $i=j$  and  $k=l$ .

### 2.5.2 PM3

Parametrized Model 3 was reported by Stewart at 1999 which is his third parameter set [47]. In this parameter set he adopted an NDDO functional, which is also identical to the AM1, and he used two Gaussian functions rather than four for per atom to employ a larger data set in evaluating the penalty function [21].

The Hamiltonian in PM3 contains the same elements as AM1 but the parameters in PM3 were derived using an automated parametrization procedure which was also devised by Stewart [20]. On the contrary the chemical knowledge and the intuition is the source to obtain the parameters in AM1. Thus, AM1 and PM3 have different values for some parameters. However, there are also some problems in PM3 model. One of them is the bonds where they are taken too short in the case of hydrogens and they are underestimated when they are between Si, Cl, Br, I. Additionally the amide bond's rotational barrier is too low and in some cases it is almost not exists, but it could be corrected by the usage of an empirical torsional potential.

## 2.6 Density Functional Theory (DFT)

The energy of a molecule could be determined by the molecule's electron density instead of a wave function and density functional theory is based on both the wave function and the electron density [19, 43, 48]. The function of an external potential energy which is acting on the density of the ground state energy of an inhomogeneous interacting many particle system is the main subject of density functional theory [49]. The earliest model for density functional was suggested by Thomas (1927) and Fermi (1927, 1928). In 1920 Dirac and in 1935 von Weizsacker

suggested the extensions of the model [48]. However the theory was firstly proposed by Kohn and Sham in 1965, but it was started to use as a computational tool for chemical problems in 1980s [50a]. In their formulation, Kohn and Sham express the electron density as a linear combination of basis functions and from these functions a determinant is formed which is called Kohn-Sham orbitals [43]. Energy is computed by using electron density from this determinant [43]. Moreover the function of electron density depends on three variables (x, y, z), but the wave function of an n-electron molecule depends on 4n variables (three spatial coordinates and one spin coordinate) [19]. Thus the most important advantage of the DFT calculations is based on its simplicity according to the ab initio methods and the calculation time while it gives the same quality [19, 50a].

The Kohn-Sham equations are similar to the standard HF equation. However the exchange term in HF is changed to the exchange-correlation potential.

The defined electronic energy of a molecule in conjunction with Kohn-Sham studies is given by the equation

$$E_e = E_v + E_T + E_J + E_{XC} \quad (2.39)$$

The first term on the right hand side of the equation (2.39) is the potential energy term while the second term defines the kinetic energy due to the electron motion.  $E_J$  term is the Coulomb repulsion between the electrons and  $E_{XC}$  term is the exchange – correlation energy [51].

Calculating the Coulomb energy of the electrons which are on their own field is hard, but assuming that they move independently and each electron experiences the field because of all electrons [50b] it could be calculated by

$$E_J = \frac{1}{2} \iint \frac{\rho(\vec{r}_1)\rho(\vec{r}_2)}{r_{12}} d\vec{r}_1 d\vec{r}_2 \quad (2.40)$$

where the  $r_{12}$  is the distance between two electrons.

The exchange correlation functionals involves the difference between classical and quantum mechanical electron-electron repulsion. In addition to the repulsion, it also contains the difference in kinetic energy between the non-interaction system and the

real system [21]. Therefore, exchange – correlation energy is defined by the following equation where  $E_{T_s}$  refers the interacting system

$$E_{XC}(\rho) = [E_T(\rho) - E_{T_s}(\rho)] + [E_{ee}(\rho) - E_J(\rho)] \quad (2.41)$$

Exchange – correlation functional is composed of two parts, the exchange part and the correlation part, hence the traditional definition of the exchange – correlational energy could be written as

$$E_{XC} = E_X + E_C \quad (2.42)$$

Due to the  $\alpha$  and  $\beta$  spin densities are contribute to give the exchange energy, exchange energy involves only the electrons of the same spin [44].

$$E_X = E_X^\alpha[\rho_\alpha] + E_X^\beta[\rho_\beta] \quad (2.43)$$

$$E_C = E_C^{\alpha\alpha}[\rho_\alpha] + E_C^{\beta\beta}[\rho_\beta] + E_C^{\alpha\beta}[\rho_\alpha, \rho_\beta] \quad (2.44)$$

where the total density is the sum of the  $\alpha$  and  $\beta$ ,  $\rho = \rho_\alpha + \rho_\beta$ , and for a closed shell singlet those are same.

Both of the exchange and correlation energies could be written in terms of energy per particle ( $\varepsilon_X$  and  $\varepsilon_C$ ) as

$$E_{XC} = \int \rho(r)\varepsilon_{XC}[\rho(r)]dr$$

$$E_{XC} = \int \rho(r)\varepsilon_X[\rho(r)]dr + \int \rho(r)\varepsilon_C[\rho(r)]dr \quad (2.45)$$

This formulation is defined as local density approximation (LDA) [52]. The exchange part of the energy density was given by Dirac exchange energy functional which is defined as

$$\varepsilon_X(\rho) = -C_X\rho(r)^{1/3}$$

$$C_X = \frac{3}{4} \left(\frac{3}{\pi}\right)^{1/3} \quad (2.46)$$

LDA indicates that the values of  $\varepsilon_{XC}$  at some position  $r$  could be calculated with  $\rho$ . Therefore, there is only one requirement for solution, a single-valued  $\rho$  at every position [21].

Constructing a gradient-corrected exchange functional to calculate accurate exchange energy was the main objective and Becke in 1988 reported a gradient corrected exchange functional as

$$E_X^{Becke}(\rho) = E_X^{LDA} - b \int \rho^{4/3} \frac{x^2}{1 + 6\beta \sinh^{-1}x} dr \quad (2.47)$$

$$x = \frac{|\nabla\rho|}{\rho^{4/3}} \quad (2.48)$$

where Becke defined  $b = 0.0042$  [53].

### 2.6.1 Hybrid functionals

One of the key features of DFT is the incorporation of correlation effects from the beginning unlike HF theory. Furthermore, if the correlation is incorporated into the HF formalism, it causes computational overhead [20]. On the other hand, HF theory provides exact means of treating exchange contribution. Thus adding a correlation energy to the HF energy which is derived from DFT could be an attractive option [20]. However this approach did not work well.

According to the Becke's strategy the exchange correlation energy could be written as

$$E_{XC} = \int_0^1 U_{XC}^\lambda d\lambda \quad (2.49)$$

The coupling parameter  $\lambda$  takes the values from 0 to 1. If it takes the value of 0, it corresponds to a system where there is no Coulomb repulsion between the electrons. Interelectronic Coulomb repulsion is involved if the value of the parameter  $\lambda$  is chosen as 1, which is also corresponds to a real system. Solving this integral could be performed by approximation by using linear interpolation

$$E_{XC} = \frac{1}{2} (U_{XC}^0 + U_{XC}^1) \quad (2.50)$$

Becke's proposition to calculate the exchange correlation energy  $U_{XC}^1$  of a fully interacting real system is the usage of local spin-density approximation.

$$E_{XC}^1 \approx E_{XC}^{LSDA} = \int u_{XC} [\rho_\alpha(r), \rho_\beta(r)] dr \quad (2.51)$$

where  $u_{XC}$  is the exchange correlation potential density. However Becke recognised that there were some problems when the parameter  $\lambda$  is chosen 0 and according to the Becke's solution the  $U_{XC}^0$  term is removed. As a result HF/DFT exchange correlation functional could be represented by involving an LSDA gradient corrected DFT expression, which is also called hybrid DFT functional [19].

Becke in 1993 developed a hybrid functional based on exchange energy functional which is called Becke3LYP or B3LYP functional [19, 54]. This functional is written as

$$E_{XC} = \int_0^1 U_{XC}^\lambda d\lambda \quad (2.52)$$

Where  $E_X^{LSDA}$  is the pure DFT LSDA non-gradient corrected exchange functional,  $E_X^{HF}$  is the KS-orbital based HF exchange energy functional,  $E_X^{Becke}$  is the Becke's exchange functional that developed at 1988,  $E_C^{VWN}$  is Vosko, Wilk, Nusair function and  $E_C^{LYP}$  is the LYP correlational functional. The  $a_0$ ,  $a_x$  and  $a_c$  parameters (typical values are  $a_0 = 0.7$ ,  $a_x = 0.2$ ,  $a_c = 0.8$ ) are those which give the best fit of the calculated energy to molecular atomization energies [19, 44]. This functional is called gradient corrected hybrid functional.

### 2.6.2 Basis Set

Atomic orbital wave functions which are based on the solution of Schrödinger equation for hydrogen atom could be used in atomic calculations. Due to the absence of a prototype species that occupies a place which is analogous to hydrogen atom, this is not convenient for molecules [19]. Solution to this problem comes from Roothaan's and Hall's studies, which points that MOs could be represented as a linear combination of basis functions [19]. The most popular way is writing each spin orbital as a linear combination of single electron orbitals [20].

$$\begin{aligned}
\psi_1 &= c_{11}\phi_1 + c_{21}\phi_2 + \dots + c_{m1}\phi_m \\
\psi_2 &= c_{12}\phi_1 + c_{22}\phi_2 + \dots + c_{m2}\phi_m \\
&\vdots \\
\psi_m &= c_{1m}\phi_1 + c_{2m}\phi_2 + \dots + c_{mm}\phi_m
\end{aligned}
\tag{2.53}$$

which is also written as

$$\psi_i = \sum_{s=1}^m c_{si}\phi_s \quad i = 1,2,3,\dots,m \tag{2.54}$$

where  $\phi_s$  represents the basis functions,  $c_{si}$  is the coefficient of the  $s^{\text{th}}$  basis function of corresponding  $i^{\text{th}}$  MO. The numbers of basis functions are represented by  $m$ .

Gaussian functions do not have a cusp at the origin and also they diminish to zero more rapidly according to the Slater functions. However unacceptable errors occur if the Slater type orbital is changed with a single Gaussian function. On the other hand, if linear combinations of Gaussian functions are used to represent the atomic orbitals, the problem would be solved [19, 20]. Therefore the linear combination has the form of

$$\phi_s = \sum_{i=1}^N d_{si}\phi_i(\alpha_{si}) \tag{2.55}$$

where  $d_{is}$  represents the coefficient of the primitive Gaussian function  $\phi_i(\alpha_{is})$  and  $N$  is the number of functions.

Thus substitution of equations (2.52) and (2.53) gives

$$\psi_i = \sum_{s=1}^m c_{si} \sum_{j=1}^N d_{sj}\phi_j(\alpha_{sj}) \quad i = 1,2,3,\dots,m \tag{2.56}$$

## 2.7 Solvation Effect

Due to the energy interactions between the solute and the solvent, the solute properties depend on vibrational frequencies, total energy and electronic spectrum which depends on the solvent. Moreover the charge separation within the molecule could be stabilized by solvent. As a result, the solvent could change the not only the

energy but also electron density [43]. Solvation effects to a structure or reaction could be visualized by adding the free energy of solvation point to point to the gas-phase PES and define another PES (Figure 2.2).

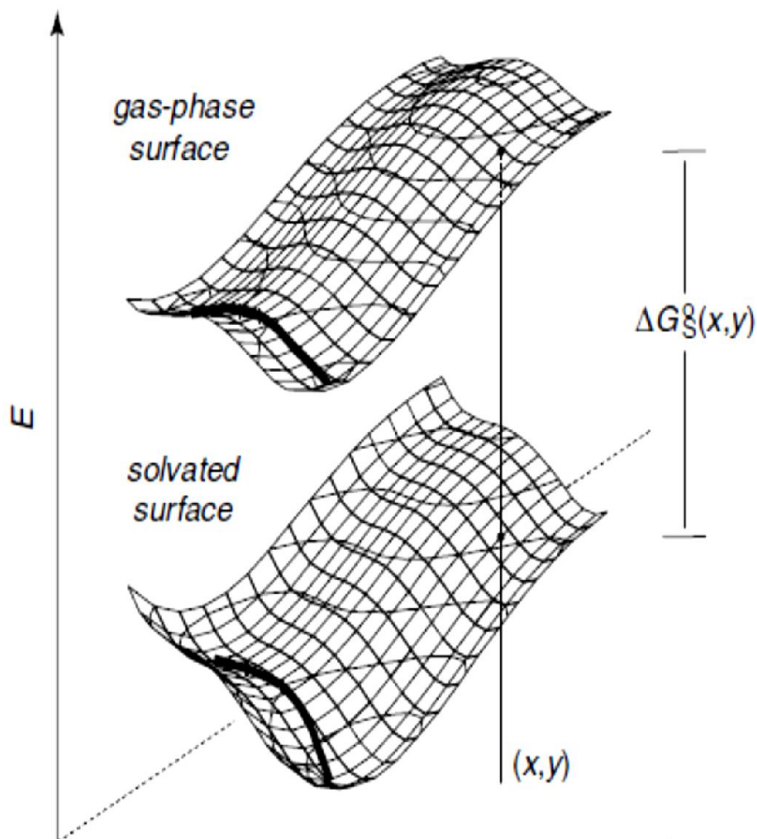


**Figure 2.2 :** A two dimensional gas-phase PES and the PES that derived from addition of solvation. Thick lines show a chemical reaction [43].

Methods to describe the effects of solvent are divided into two types. One of them describes the individual solvent molecules and the other kind treats the solvent as a continuum medium. Moreover, combinations of these kinds are also possible. These kinds could be also divided according to the usage of the classical or the quantum mechanical description. On the other hand, solvent effects could be divided into two parts as specific solvation and short-range effects.

Cavitation energy, which is one of the effects that occurs where the molecule meets the solvent shell, is the required energy to push aside the solvent molecules. Force attraction is another solvent effect which occurs due to the van der Waals, dispersion and hydrogen bonding interactions [43].



### 2.7.1 Polarized continuum models

Surface boundary approach is a kind of implementation of Poisson equation which was first formalized by Miertus, Scrocco and Tomassi in 1981. This formalization is called polarized continuum model (PCM) [21].

PCM manage the van der Waals surface type cavity and parametrizes the cavity/dispersion contributions based on the area of the surface.

The non-linear Schrödinger equation according to the quantum mechanical continuum models have the formulation of

$$\left(H - \frac{1}{2} V\right) \Psi = E\Psi \quad (2.57)$$

where V is the general reaction field inside the cavity which depends on wave function. If wave function is expressed as a Slater determinant the orbitals that minimizes the Schrödinger equation could be derived from [21].

$$(F_i - V) \psi_i = e_i \psi_i \quad (2.58)$$

where F is the Fock operator.

The difference between the energy in gas phase and the energy in solution gives the electrostatic component of the solvation

$$\Delta G_{ENP} = [\langle \Psi^{sol} | H | \Psi^{sol} \rangle + \langle \Psi^{sol} | G_P | \Psi^{sol} \rangle] - \langle \Psi^{gas} | H | \Psi^{gas} \rangle \quad (2.59)$$

$$\Delta G_{ENP} = \Delta E_{EN} + G_P \quad (2.60)$$

where  $\Delta E_{EN}$  is the distortion energy and EN term is associated with the electronic and nuclear components of the total energy [21]. According to PCM model cavity creation in the medium needs energy and electric charge distribution polarize the medium. Therefore the free energy of the solvation is calculated by [44].

$$\Delta G_{solvation} = \Delta G_{cavity} + \Delta G_{dispertion} \Delta G_{electrostatic} \quad (2.61)$$

Choosing the cavity as spherical is the simplest reaction field model where only the dipole moment and the net charge are considered while the cavity/dispersion effects are ignored. Thus Born model is given by [44]

$$\Delta G_{el}(q) = - \left(1 - \frac{1}{\varepsilon}\right) \frac{q^2}{2a} \quad (2.62)$$

where  $q$  is the net charge,  $a$  is the radius of cavity,  $\varepsilon$  is the dielectric constant.

## 2.8 Population Analysis

Partitioning the wave function or the electron density into charges on the nuclei and bond orders are performed by a mathematical way which is called population analysis. The results that are obtained from population analysis are those which can not be observed by experiments. For example due to the lack of physical property, atomic charges could not be observed experimentally. On the other hand abstraction of electron density and the nuclear charges on each atom to partial charges is helpful to understand electron density distribution [43]. Thus, predicting the sites where nucleophilic or electrophilic attack could occur would be easy to predict.

### 2.8.1 Natural Bond Order (NBO) Analysis

Natural bond order analysis involves a set of analysis techniques. Natural population analysis is one of them and it is performed to obtain occupancies and charges NBO uses natural orbitals instead of molecular orbital [43]. The eigenfunctions of first order which reduces density matrix are the natural orbitals [43]. Natural orbitals could be used to derive atomic charges and molecular bonds by distribute the electrons into atomic and molecular orbitals. The shape of the atomic orbitals is defined by the one electron density matrix by performing Natural Atomic Orbital and Natural Bond Orbital analysis [44].

The electron density is calculated from the wave function by

$$|\Psi|^2 = \Psi * \Psi \quad (2.63)$$

Therefore the reduced density matrix of order  $k$ ,  $\gamma_k$ , is defined by

$$\begin{aligned} & \gamma_k(r'_1, r'_2, \dots, r'_k, r_1, r_2, \dots, r_k) \\ &= \binom{N}{k} \int \Psi^*(r_1, r_2, \dots, r_k, r_{k+1}, \dots, r_N) \Psi(r_1, r_2, \dots, r_k, r_{k+1}, \dots, r_N) dr_{k+1} \cdot \end{aligned} \quad (2.64)$$

The integration of first order density matrix over the coordinate 1, yields the number of electrons. The first order density matrix could be diagonalized and Natural

Orbitals and Occupation Numbers could be found [43]. The occupation number of the natural orbitals could be either 0 or 2.

The first step in NBO analysis is localization of natural atomic orbitals which are associated almost entirely with a single atom [21]. The second step involves the localization of orbitals that contains bonding/antibonding between pairs by the usage of the basis set AOs of the corresponding atoms [21, 43]. The last step in analysis is, identification of Rydberg-like orbitals and orthogonalization of orbitals with each other [21, 43]. Therefore, all of the NAOs (and also Rydberg orbitals) are described by the basis set AOs of a single atom and all of the NBOs are described by the basis set AOs of two atoms [21]. Moreover, characterization of three center bonds would be performed by decomposition into three body orbitals.

## **2.9 Potential Energy Surface (PES) and Conformational Analysis**

Potential energy surface (PES) is a kind of graphical representation of the Born-Openheimer (BO) potential energy function that links key chemical concepts and basic geometrical features of any given molecule, molecular complex or a chemical reaction [50c]. The minima of a potential energy surface is the minimum energy conformations and the saddle points are the transition state. For this reason both of the minima and the saddle points are really important. The local minimum which represents the minimum energy conformation is defined by the atomic arrangements where the gradient of potential energy function vanishes [50c]. On the other hand saddle points are like the top of a mountain that would be passed from one valley to another [50c].

Small distortions not only in bond angles but also in the bond lengths cause the interconversion of the arrays of the atoms of a molecule which determines the conformations of that molecule [20, 50d]. Furthermore three dimensional structures of a molecule, define the physical, chemical and also biological properties of a molecule [50d]. In biochemical researches determining a protein structure is important, thus finding the lowest energy conformer, which is the most stable conformer, is also important. In order to find the lower energy shape of geometry a local minimum of the conformer should be found [43, 50e]. Besides the conformational differences are really important drug chemistry due to the importance

of using the lowest energy conformer to prevent the deformations from the conformations [50d].

Determining the most stable conformations and transition states between the conformers could be analyzed by conformational search [50e]. The aim of a conformational analysis is identifying the dynamics of atomic motion characteristic of the conformational behavior of a molecule [50c]. Conformations of a molecule involve all of the low energy minimas on the PES. Therefore the conformational search could be referred as searching the local minimas or the low energy saddle points on the PES [50c]. Moreover the conformational analysis could be referred as the study about the conformations which affect a molecule's properties [20, 50d]. Although the earliest and the simplest conformational ideas have been performed by Sachse and Bischoff in 1890, the modern conformational analysis has been developed by D. H. R. Barton at 1950 [20, 50d, 55].

Energy minimizations have a big role in conformational analysis. That's why having a separate algorithm is necessary to find the minimas on energy surface [20]. The energy of conformations could be calculated by ab initio, semiempirical and also MM methods. The method that is chosen to calculate the conformational energy is depends on not only the size of the molecule but also the required accuracy of the energies according to the availability of parameters [50e]. On the other hand, there could be lots of minimas on a energy surface while the Boltzmann function ( $K = \exp(\Delta G/RT)$ ) controls the distribution of the conformers of a conformational space [20, 50d]. In that case it is preferred to find all the accessible minimas [20].

## 2.10 Computational Details

The conformer analysis for the PLP-Methylamine and D-Tryptophan Methyl Ester model structure performed at PM3 level of theory using Spartan 04 programme [47, 56]. The first five lowest energy structures selected for further optimization. All of the structures; reactants, intermediates, transition states and products along the reaction path are optimized at the B3LYP/6-31+G(d,p) using Gaussian 09 programme [57]. The model compound and the intermediates formed along the reaction coordinate are charged species. Therefore, diffused functions are added to the basis set. Since the path is included proton transfers, addition of one set of p primitives to hydrogen atoms is inevitable. Once the lowest energy conformer for

PLP – D-TrpMe and PLP-5-HT complex is determined, the proposed reaction mechanisms modeled starting from this conformer. To observe the charge distribution on the structures the NBO analysis performed. The solvent effect is calculated with Integral Equation Formalism PCM (IEFPCM) methodology as implemented in G09 at 6-31+g(d,p) level of theory with full optimization [58]. Water ( $\epsilon=78.39$ ) was used as a solvent in order to mimic the highly and moderately polar types of surroundings of the active site. The molecular cavity is build up with UFF radii which uses UFF force field. By choosing this model, a sphere around each solute atom with the radii scaled by a factor of 1.1 placed where the explicit hydrogens have individual spheres.



### 3. RESULTS AND DISCUSSION

The two proposed mechanism for transformation reactions of DDC have several parts: formation of external aldimine, formation of quinonoid and ketimine formation. The internal aldimine, a PLP Schiff base with an amino group of Lys303 residue, is converted to the external aldimine, a new PLP Schiff base with the enzyme (Figure 3.1, a, b, structure 3). In literature, the external aldimine formation is also known as transimination. In the second step the external aldimine is converted to experimentally observed quinonoid structure (Figure 3.1, a, b, structure 4) by proton abstraction. At last the ketimine structure is formed from the quinonoid via proton transfer (Figure 3.1, a, b, structure 5).

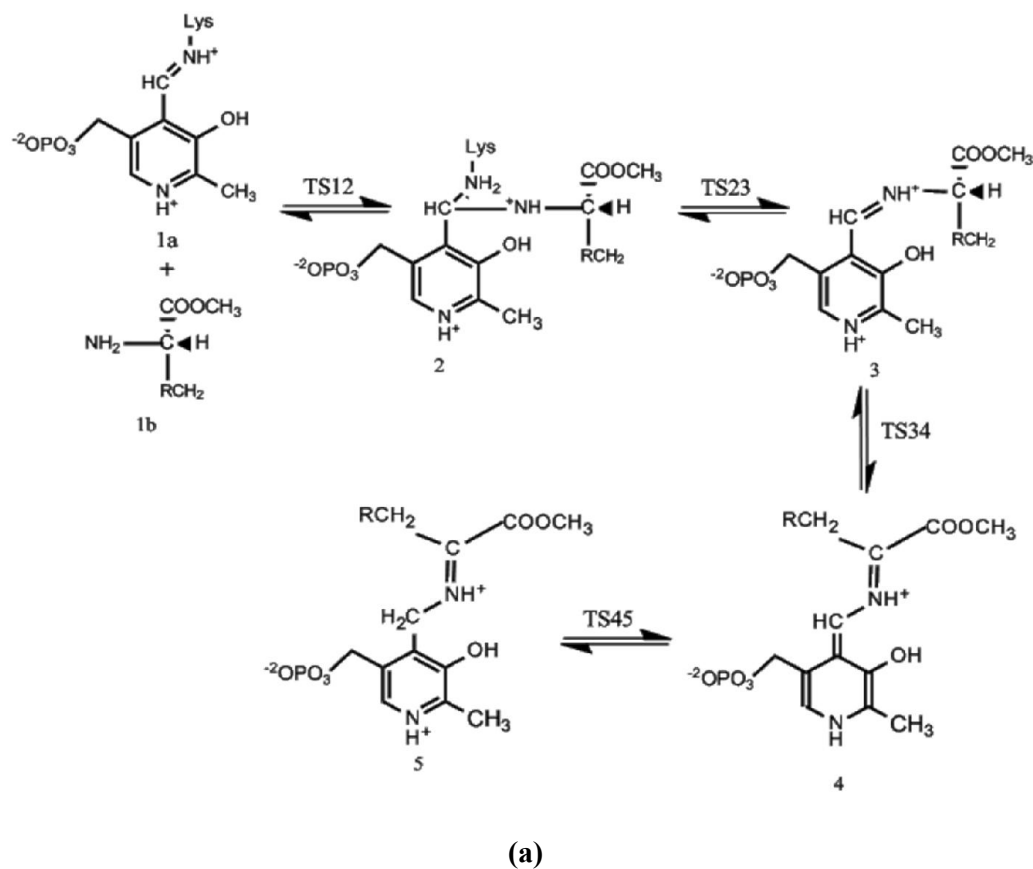


**Figure 3.1 :** Schematic representation of half transamination mechanisms of DDC with D-tryptophan methyl ester. a) Reaction path of PLP-5 - D-tryptophan methyl ester complex.

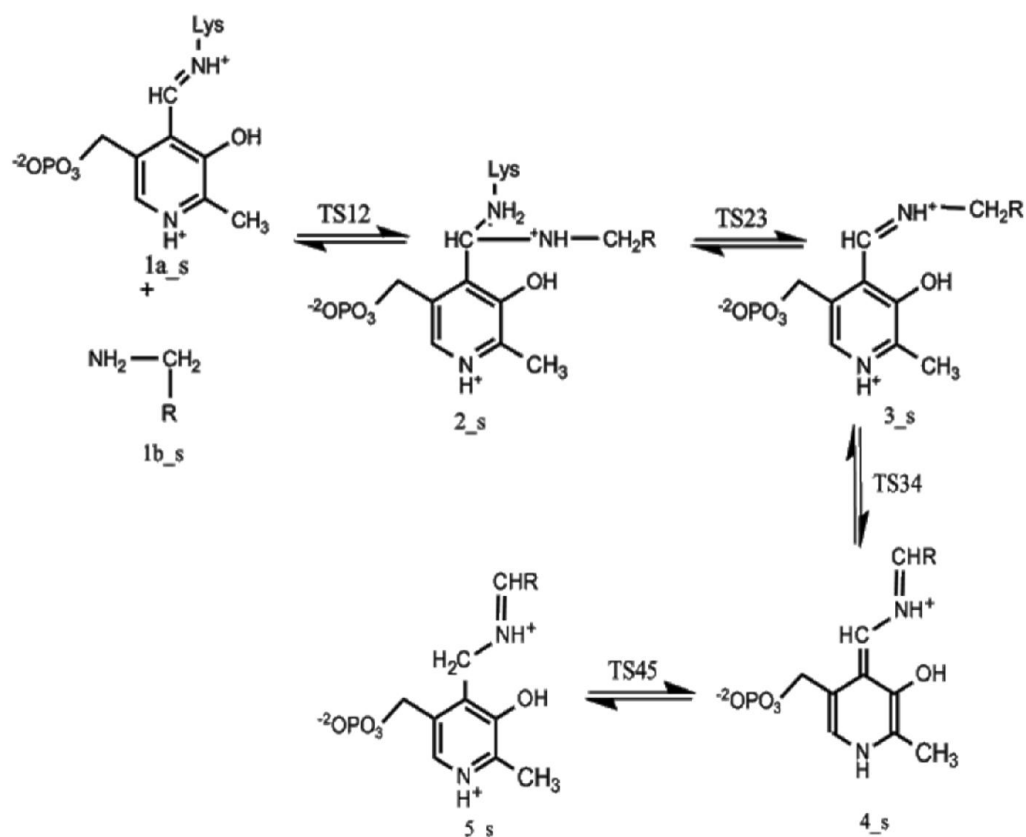


**Figure 3.1 (continued):** Schematic representation of half transamination mechanisms of DDC with D-tryptophan methyl ester. **b)** Reaction path of PLP-5-HT complex.

Based on the experimental results 5-HT works as a mechanism based inactivator for DDC enzyme [39]. It is known that 5-HT can be used to prevent massive consumption of D-TrpME therefore we choose them to compare the activation energy barriers to validate the activity difference between them.

### 3.1 Model Structures

In order to mimic the transamination mechanism of DDC with 5-HT and D-tryptophan methyl ester, model structures are used. In this study Lysine303 (Lys303), attached to PLP, has been represented as a methylamine (Figure 3.2a). This method of representing PLP dependent enzymes is common and widely accepted in literature [58, 59, 60]. Also, the phosphate group on PLP was replaced with a methyl group which is also widely used application (Figure 3.2b) [10, 12, 58, 59, 60]. Based on the crystal structure studies it can be stated that the carboxyl group lies perpendicular to the plane of the PLP ring [21].



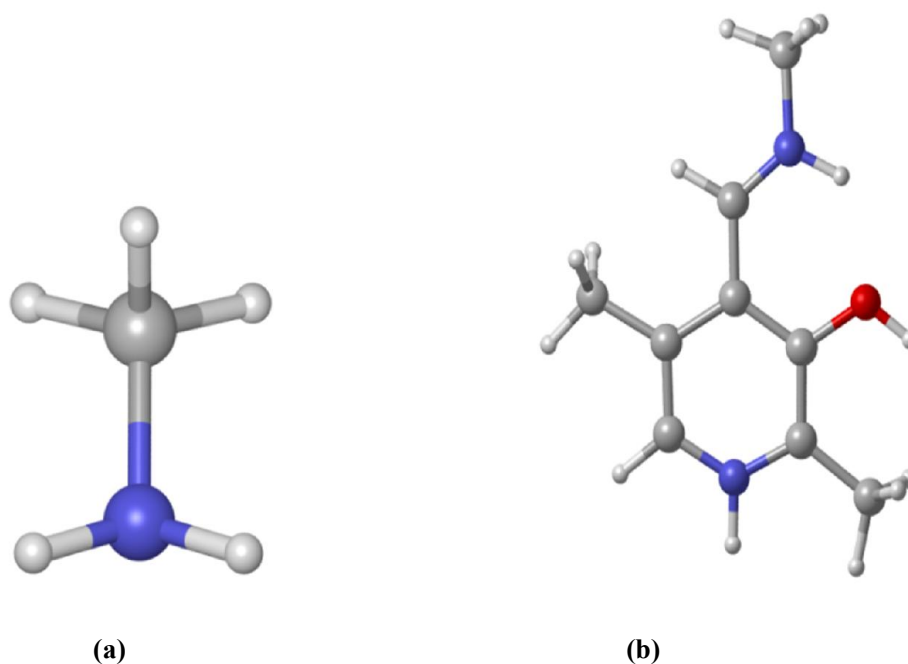


**Figure 3.2 :** Three dimensional geometries of model structures. a) Methylamine as Lys303. b) PLP-methylamine complex as PLP-Lys303 complex.

### 3.2 Conformational Analysis

Conformational analysis was performed for the 4'-N-protonated internal aldimine (structure 1a), D-tryptophan methyl ester using semiempirical method PM3 implemented in the Spartan 04 programme. The first five lowest energy conformers were chosen for further optimization at high level of theory. The frequency and energy calculations for these conformers has been performed with B3LYP/6-31+G(d,p) level. The two lowest energy for 4'-N-protonated internal aldimine conformers are depicted in Figure 3.3. The energy difference between the two lowest energy conformers is found to be 4.5 kcal/mol. The main structural difference between these conformers is the position of methylamine that is used for mimicking Lys303 residue. The angle N2 – H10 – C10 has a value of 127.05° and the distance of 1.942 Å between H10 on the methylamine group and O1 generates H-bonding interaction in the lowest energy conformer. However, for the second lowest energy conformer the angle changes to 48.2° and the distance between H10 and O2 is about 4.44 Å does not allow H-bonding interaction within the structure. To provide more steric effect on active side residues, ethyl was used rather than to methyl for mimicking phosphate group.

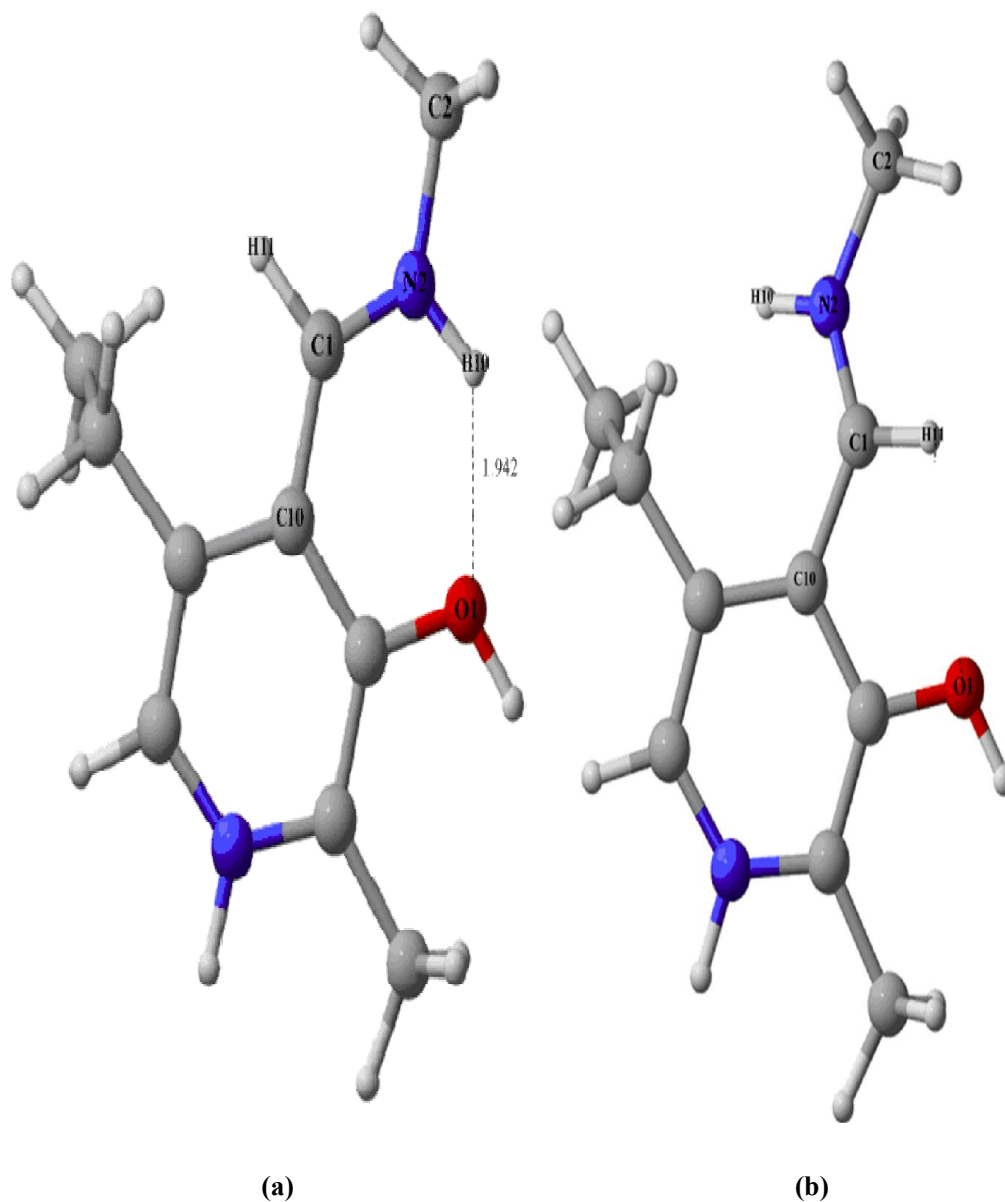


**Figure 3.3 :** Three dimensional geometries of optimized (B3LYP/6-31+G(d,p)) geometries of 4'-N-protonated internal aldimine. a) The lowest energy conformer. b) The second lowest energy conformer.

The two lowest energy for D-tryptophan methylester (structure 1b) and 5-HT (structure 1b\_s) conformers are depicted in Figure 3.4 respectively. The energy difference between the two lowest energy of D-tryptophan methylester conformers is found to be about 1.3 kcal/mol. The main structural difference between these conformers is the position of carboxyl group. It can be stated that, despite the stabilizing effect of H-bonding interactions between carboxyl group O2 and H1 on the N1 for both structure, the steric hindrance destabilizes the second structure with respect to the previous one.

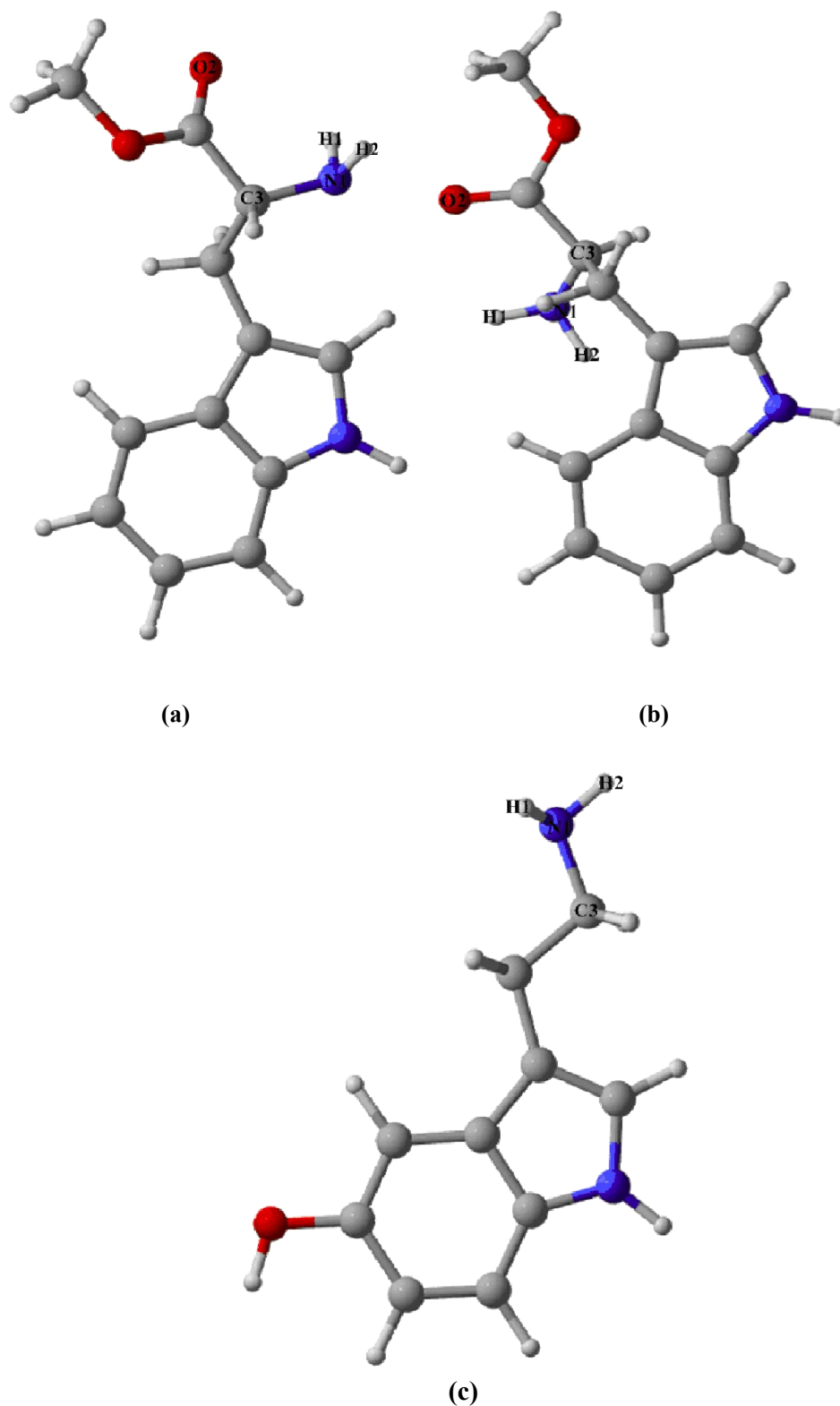


**Figure 3.4 :** Three dimensional geometries of optimized (B3LYP/6-31+G(d,p)) geometries of D-tryptophan methylester and 5-HT conformers a) The lowest energy conformer of D-tryptophan methylester. b) The second lowest energy conformer of D-tryptophan methylester. c) The lowest energy conformer of 5-HT.

### 3.3 D-tryptophan Methyl ester

#### 3.3.1 External aldimine formation

All known PLP enzymes have a Schiff base (internal aldimine) and an active site lysine residue in their resting state. The incoming, amine-containing substrate displaces the lysine amino group from the internal aldimine, in the process forming an external aldimine. External aldimine formation starts with the formation of PLP-substrate complex as Lys – 303 leaves the PLP. The formation of a bond between C1 of PLP and N1 of substrate and a proton transfer from N1 of substrate to N2 of PLP occurs simultaneously. In the transition state, TS12, the N1-C1-N2 angle is 94.80° and the N1-C1 distance is 1.509 Å. In addition, the N1-H1 and N2-H1 distances are 1.318 Å, 1.347 Å respectively. The transition state structure (TS12) is determined with one imaginary frequency having a value of -1617.89. The relative free energy barrier for the transition state (TS12) is found to be 20.1 kcal/mol which is more stable relative to the previous work that has 23.7 kcal/mol for similar transition state [60]. The transition state (TS12) was also validated with intrinsic reaction coordinate (IRC) calculations. The reverse IRC calculation produced an intermediate structure namely methylamine – PLP – substrate complex instead of the two reactants. (Figure 3.4a) The energy of the complex structure is -16.6 kcal/mol relative to the separated reactants because of the stabilizing effect of the H-bonding interactions within the complex. The intermediate structure 2 obtained from IRC calculations has an energy value of -22.0 kcal/mol. Angle between N1-H1-O2 is about 113.20° for the complex while it is about 52.50° for structure 2. It can be also stated that, the strong H-bonding interactions within the active site residues such as H1 - O2 and the other H on the N2 - O1 provide stabilizing effect for the structure 2.

In literature stepwise mechanism is proposed for the External Aldimine formation. At second part of the External Aldimine formation, Lys-303 should leave from the PLP and a stable structure should be achieved for further parts. A transition state cannot be located due to the presence of strong electrostatic interactions within the molecule. D-TrpME has a carboxylic group which is located on  $\alpha$ -C atom and it has interactions with the surrounding amino acid residues in the enzyme. However, because of the size of model structure, the carboxylic group cannot be stabilized.



In order to understand the geometrical dynamics of the transition state, the carboxyl group is replaced by the methyl and then a transition state TS23 can be optimized. It should be also noted that, the same transition state is located in the presence of 5-HT which the details will be given in following sections.

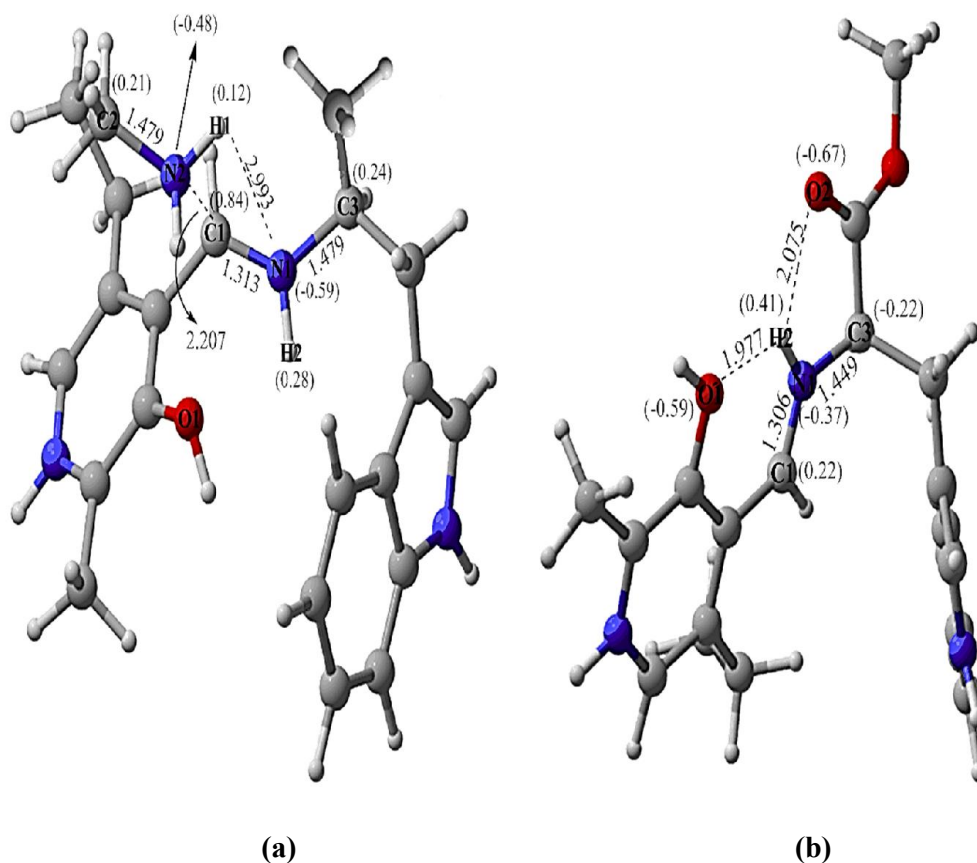


**Figure 3.6 :** a) Transition state (TS23) of PLP D-tryptophan methylester model complex. b) Geometry optimization result from forward IRC calculation. (Structure 3, 4'-N-protonated external aldimine)

In the transition state, TS23, the N1-C1-N2 is 108.00 and the N1-C1 distance is 1.313 Å. In addition, the C1-N2 and N1-C3 distances are 2,207 Å, 1,479 Å respectively. The transition state structure (TS23) is determined with one imaginary frequency having a value of -51.89. The transition state (TS23) was also validated with intrinsic reaction coordinate (IRC) calculations. The forward IRC calculations pointed out 4'-N-protonated external aldimine (structure 3) (Figure 3.6b). The relative free energy value is found to be 14.0 kcal/mol for the representative of the TS23. Therefore the free energy value of the TS23 bearing a carboxyl group is expected to have a value lower than 14.0 kcal/mol.

### 3.3.2 Quinonoid Formation

Based on the experimental findings, formation of intermediate quinonoid structure (Figure 3.7c) could be detected during the oxidative deamination and transamination reactions catalyzed by DDC. According to Bertoldi et al. the rate of formation and degradation of the quinonoid species indicates that this is not rate limiting step [40]. Therefore, these experimental findings, that are consistent with our calculations at least up to the formation of a stable quinonoid structure. The stepwise mechanism is modeled with the assistance of either water or Threonine which is chosen due to its closeness to the active site. The transition state TS34 assisted by water, has an energy barrier of 30.4 kcal/mol, results the transformation of the C3-N1 single bond with the distance 1.448 Å to double bond with the distance of 1.325 Å and C1-N1 double bond with the distance 1.306 Å to partial double bond with the distance 1.361 Å. The transition state structure (TS34) is determined with one imaginary frequency having a value of -334.37. By the help of interaction between bonding and antibonding orbitals of C4 with the proton H4 and the stabilizing effect of H-bonding between O2-H2 and O1-H2 facilitate the proton transfer (H3) from C3 to water.

The stepwise mechanism was also studied with the assistance of Threonine. The transition state TS34 assisted by threonine, has an energy barrier of 57.1 kcal/mol, also results the transformation of the C3-N1 single bond to double bond and C1-N1 double bond to partial double bond. Proton transfer from C3 to threonine is also achieved at this step (Figure 3.7b). However, the transition state assisted by threonine requires more free energy than the water assisted mechanisms. As a result of gas phase calculations, the water assisted mechanism is found to be the most plausible mechanism for the formation of quinonoid and later steps.

### 3.3.3 Ketimine Formation

Ketimine formation is provided by proton transfer from water to C1 of PLP. In this step H3 is transferred to the C1 of the PLP at a O3-H3 distance of 1.519 Å and H3-C1 distance of 1.239 Å (TS45, Figure 3.8a). While the proton transferred to C1, the partial double bond with distance of 1.361 Å between C1-N1 turns to the single bond having a value of 1.480 Å. Moreover the bond length between N1-C3 changes from 1.325 Å to 1.294 Å. This proton transfer and double bond shift leads to the formation of ketimine structure.

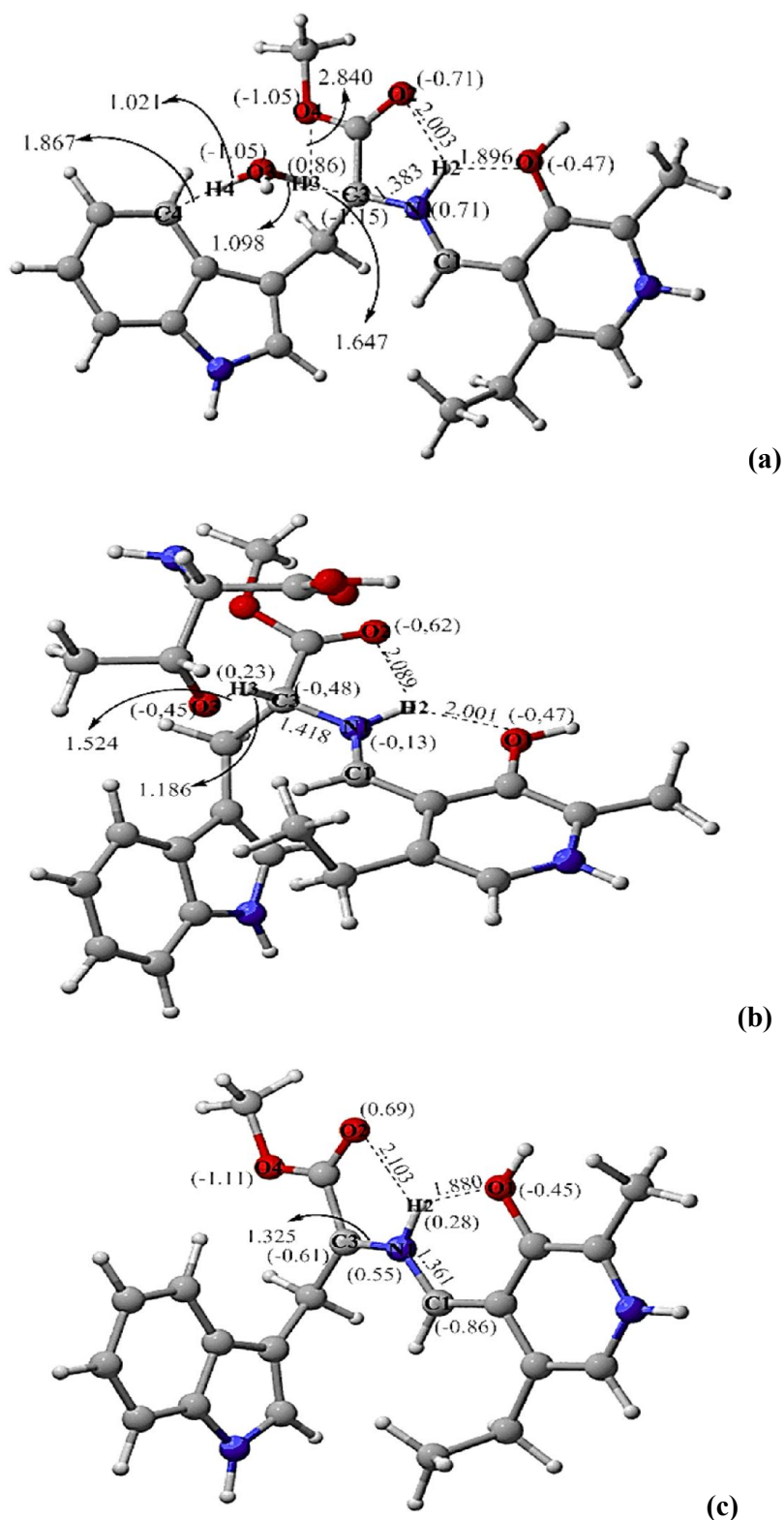


**Figure 3.7 :** Three dimensional geometries of formation of quinonoid (structure 4).  
 a) Transition state (TS34) with water assistance. b) Transition state (TS34) with Threonine assistance. c) Geometry optimization result from forward IRC calculation. (structure 4, quinonoid).





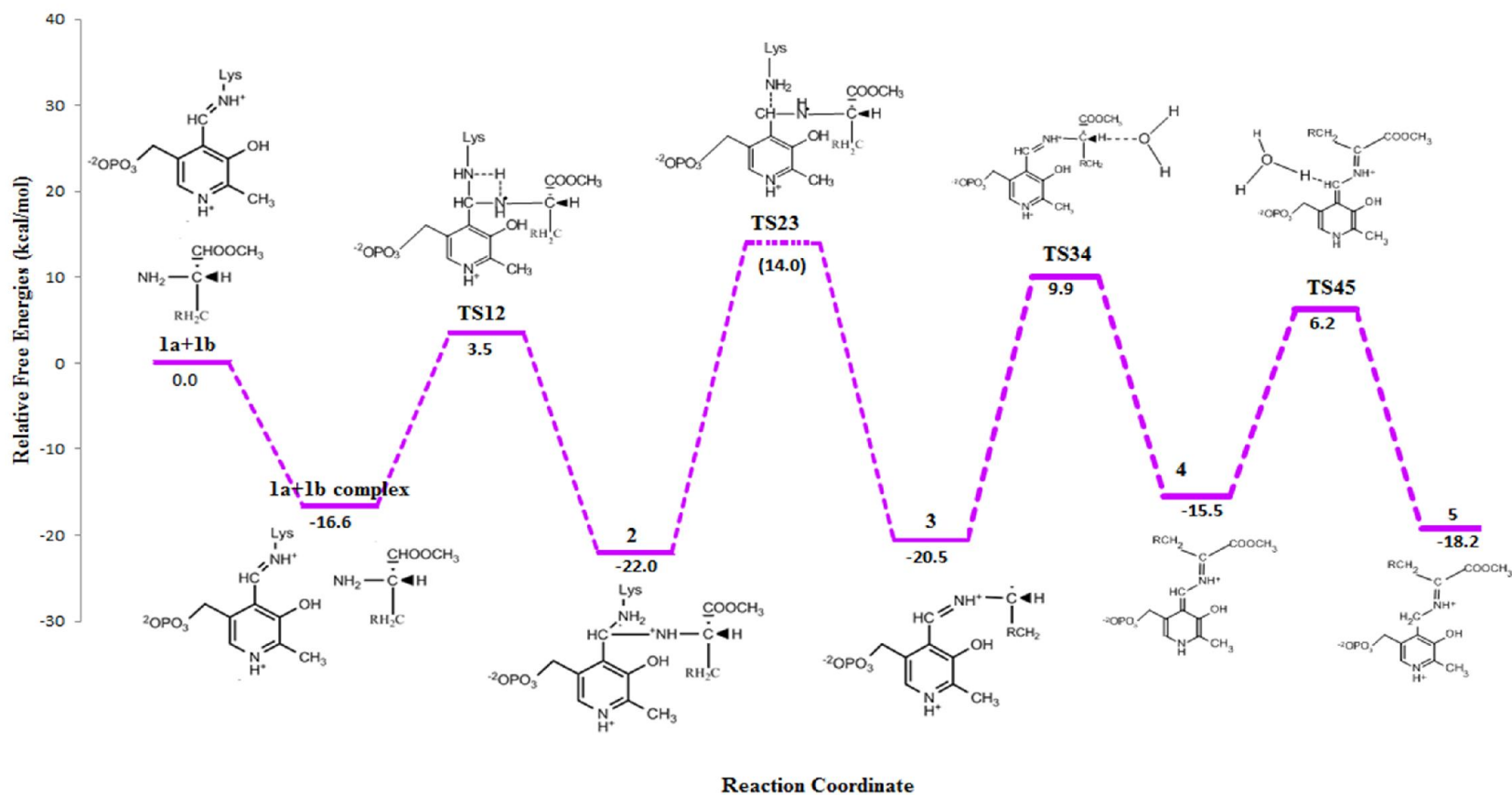


**Figure 3.9** : Energy profile for D-TrpME - DDC mechanism in gas phase. Relative free energies are given as kcal/mol

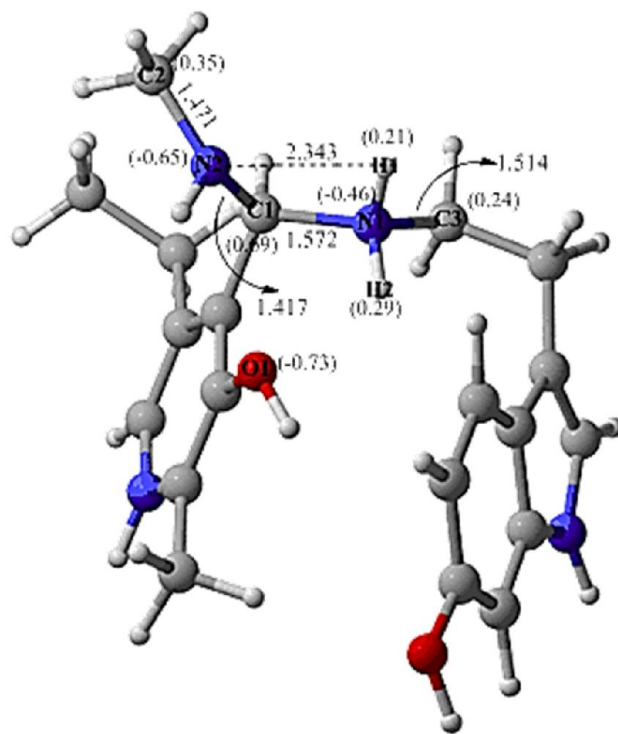
### 3.4 5-Hydroxy Tryptophan (Serotonin)

#### 3.4.1 External aldimine formation

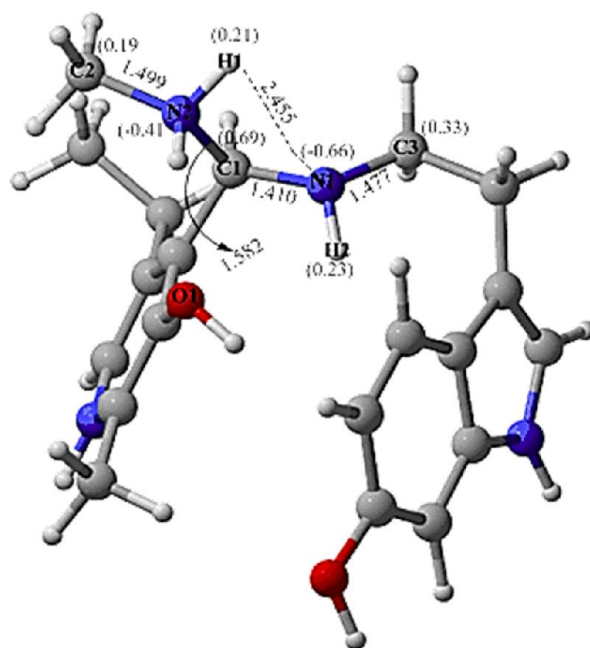
A mechanism based inactivator of DDC enzyme, 5-HT (serotonin) is also modeled for side reactions. Serotonin has several structural difference relative to the D-TrpME. Our main concern to identify the effect of the carboxyl group on the  $\alpha$ -Carbon. It should be also noted that there are several kinetic studies which can be used as a validation for the details of the reaction mechanism we studied.

In the transition state, TS12\_s, the N1-C1-N2 is the same as in TS12 for D-TrpMe (Figure 3.1c) value of 94.80 and the N1-C1 distance is 1.503 Å. In addition, the N1-H1 and N2-H1 distances are 1,341 Å, 1,319 Å respectively. The transition state structure (TS12\_s) is determined with one imaginary frequency having a value of -1600.66. According to geometrical details of TS12 and TS12\_s, it can be stated that there is no significant changes in transition state geometries. However carboxyl group on the  $\alpha$ -Carbon is replaced with hydrogen atom, thus the free energy of TS12\_s is much more than the TS12 due to the existence of stabilizing effect of H-bonding interactions in TS12. The transition state (TS12\_s) was also validated with intrinsic reaction coordinate (IRC) calculations. The reverse IRC calculation produced an intermediate structure namely methylamine – PLP – substrate complex instead of the two reactants (Figure 3.10a). The energy of the complex structure is -15.6 kcal/mol relative to the separated reactants which is also bigger than the complex structure obtained from D-TrpME studies. The intermediate structure 2\_s obtained from IRC calculations has a an energy value of -14.4 kcal/mol. Angle between N1-H1-N2 is about 75.50 for the complex while it is about 81.80 for structure 2. It can be also stated that, the H-bonding interactions within the active site residues such as H2 – O1 which has a value of 2.136 Å in complex while has a value of 2.556 Å in structure 2\_s provide more stabilizing effect for the complex structure (Figure 3.10b).

5-HT has not a carboxylic group on its  $\alpha$ -C atom thus the interactions with the surrounding atoms in the active site is weaker than the D-TrpME. Therefore, the methylamine group left the complex easier due to the absence of strong interactions in the active site. In the transition state, TS23\_s, the N1-C1-N2 is 108.0<sup>o</sup> and the N1-C1 distance is 1.313 Å.

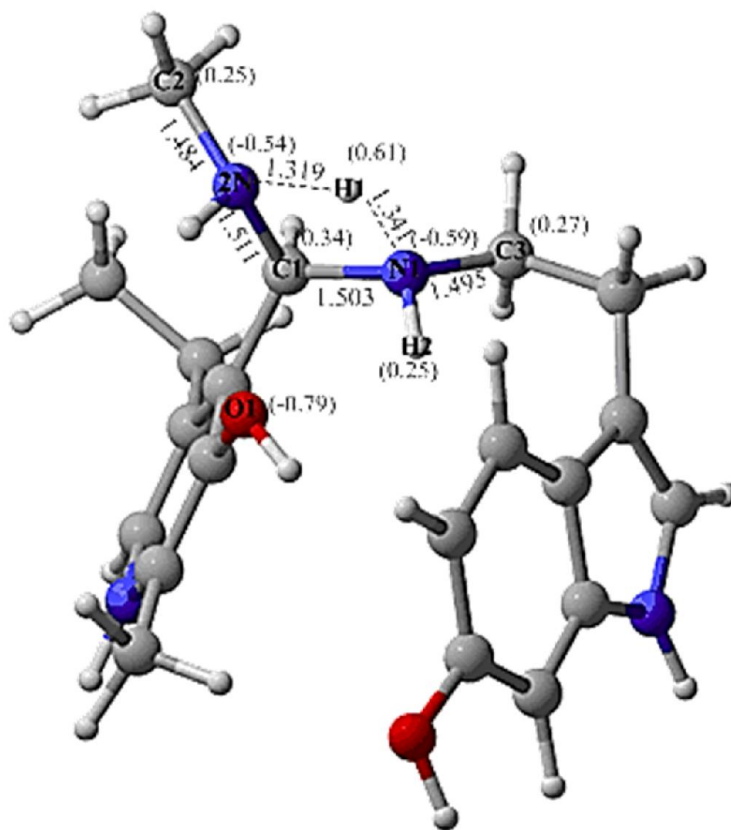


(a)



(b)

**Figure 3.10 :** Three dimensional geometries of formation of 5-HT complex (structure 2\_s). a) Structure 1a\_-1b\_s Complex before transition state formation. b) Geometry optimization result from forward IRC calculation.



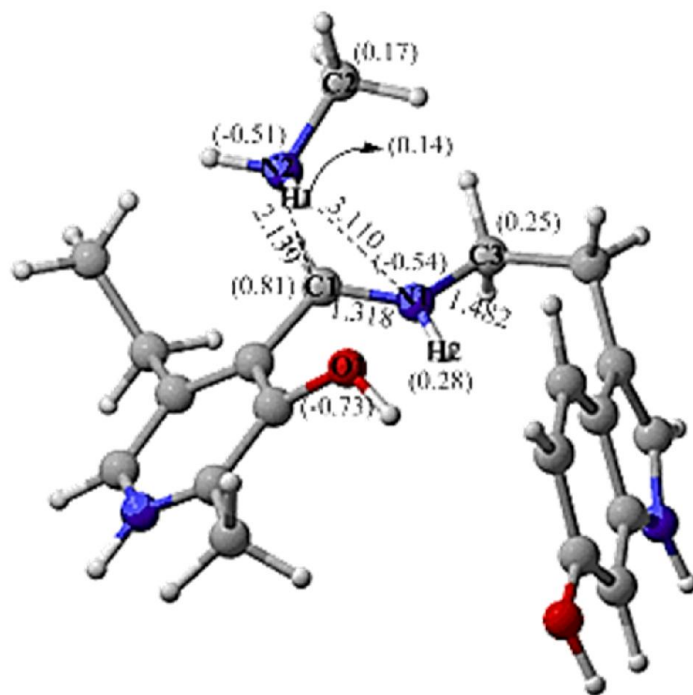
(c)

**Figure 3.10 (continued):** Three dimensional geometries of formation of 5-HT complex (structure 2\_s). c) Transition state (TS12\_s) of PLP 5-HT complex.

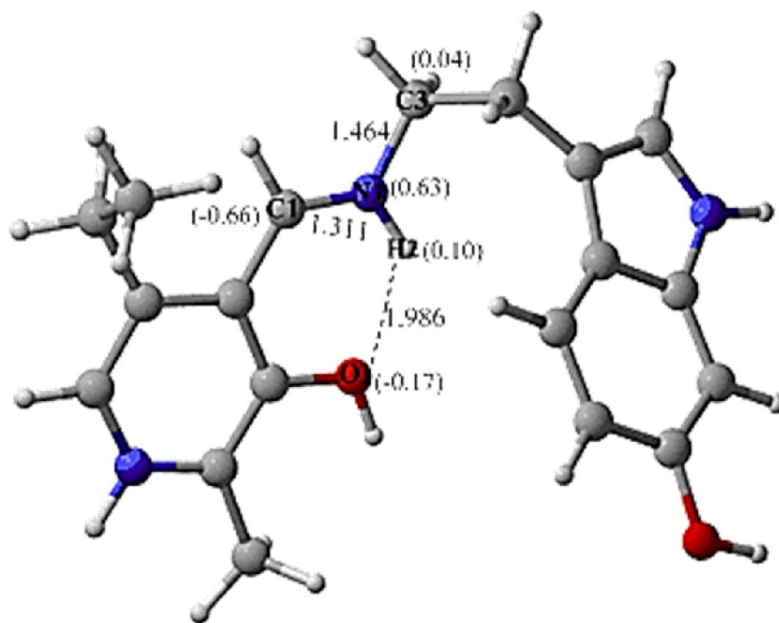
In addition, the C1-N2 and N1-C3 distances are 2.207 Å, 1.479 Å respectively. The transition state structure (TS23\_s) is determined with one imaginary frequency having a value of -51.89. The transition state (TS23\_s) was also validated with intrinsic reaction coordinate (IRC) calculations. The forward IRC calculations pointed out 4'-N-protonated external aldimine (structure 3\_s) (Figure 3.11b)

### 3.4.2 Quinonoid Formation

As in the D-TrpMe the stepwise mechanism is modeled with the assistance of water. The transition state TS34\_s assisted by water, has an energy barrier of 30.7 kcal/mol, results the transformation of the C3-N1 single bond with the distance 1.420 Å to double bond with the distance of 1.311 Å and C1-N1 double bond with the distance 1.312 Å to partial double bond with the distance 1.386 Å.



(a)



(b)

**Figure 3.11** : a) Transition state (TS23\_s) of PLP 5-HT complex. b) Geometry optimization result from forward IRC calculation. (structure 3\_s, 4'-N-protonated external aldimine)

The transition state structure (TS34\_s) is determined with one imaginary frequency having a value of -342.89. The transition state (TS34\_s) was also validated with intrinsic reaction coordinate (IRC) calculations. The forward IRC calculations pointed out quinonoid structure (structure 4\_s) (Figure 3.12b)

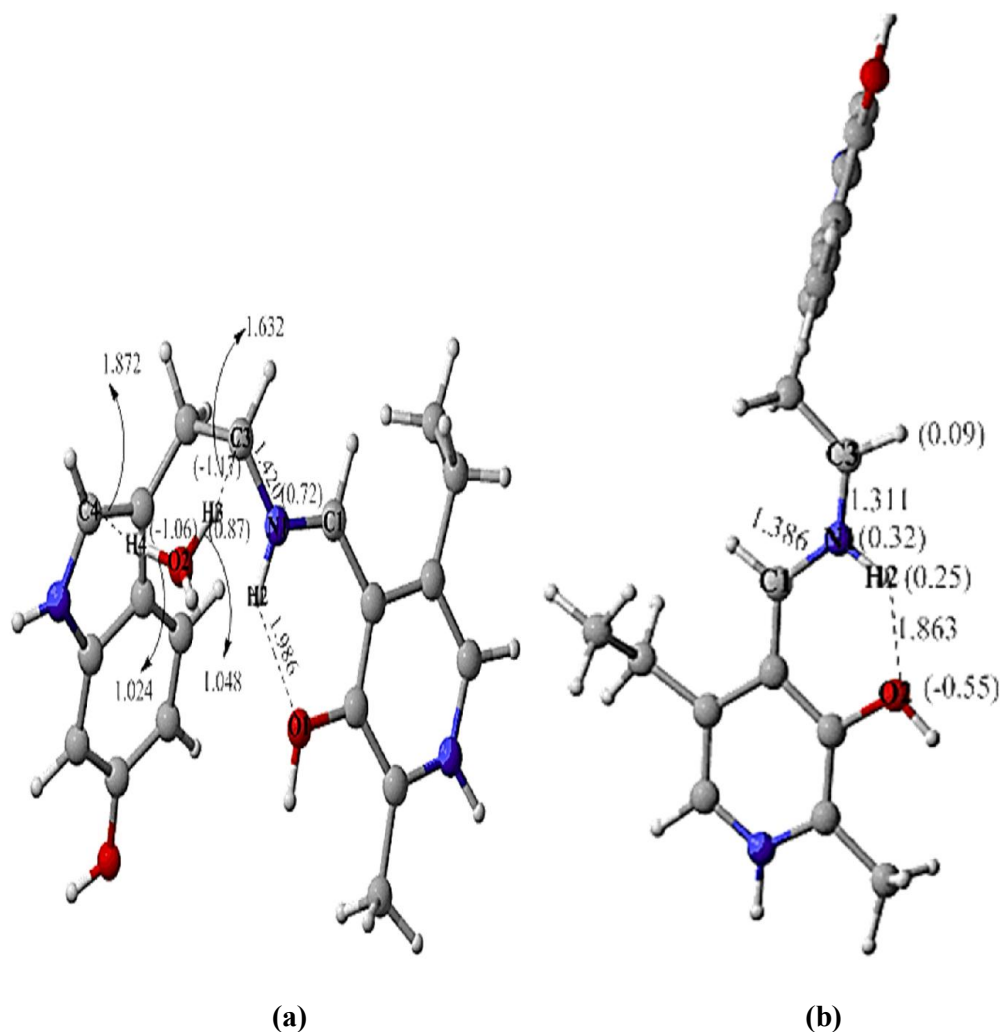


**Figure 3.12 :** Three dimensional geometries of formation of quinonoid (structure 4\_s). a) Transition state (TS34\_s) with water assistance. b) Geometry optimization result from forward IRC calculation. (structure 4\_s, quinonoid)

### 3.4.3 Ketimine Formation

Ketimine formation is provided by proton transfer from water to C1 of PLP. In this step H3 is transferred to the C1 of the PLP at a O3-H3 distance of 1.519 Å and H3-C1 distance of 1.239 Å (TS45, Figure 3.13a). While the proton transferred to C1, the

partial double bond with distance of 1.361 Å between C1-N1 turns to the single bond having a value of 1.480 Å. Moreover the bond length between N1-C3 changes from 1.325 Å to 1.294 Å. This proton transfer and double bond shift leads to the formation of ketimine structure. Relative free energy barrier for this transition state is found to be 21.7 kcal/mol. A stable geometry of ketimine is provided by the further IRC calculations. As previous structure H-bonding interactions between O1-H2 and O2-H2 provide stabilizing effect of ketimine structure which has a relative free energy of -18.2 kcal/mol (Figure 3.13b).

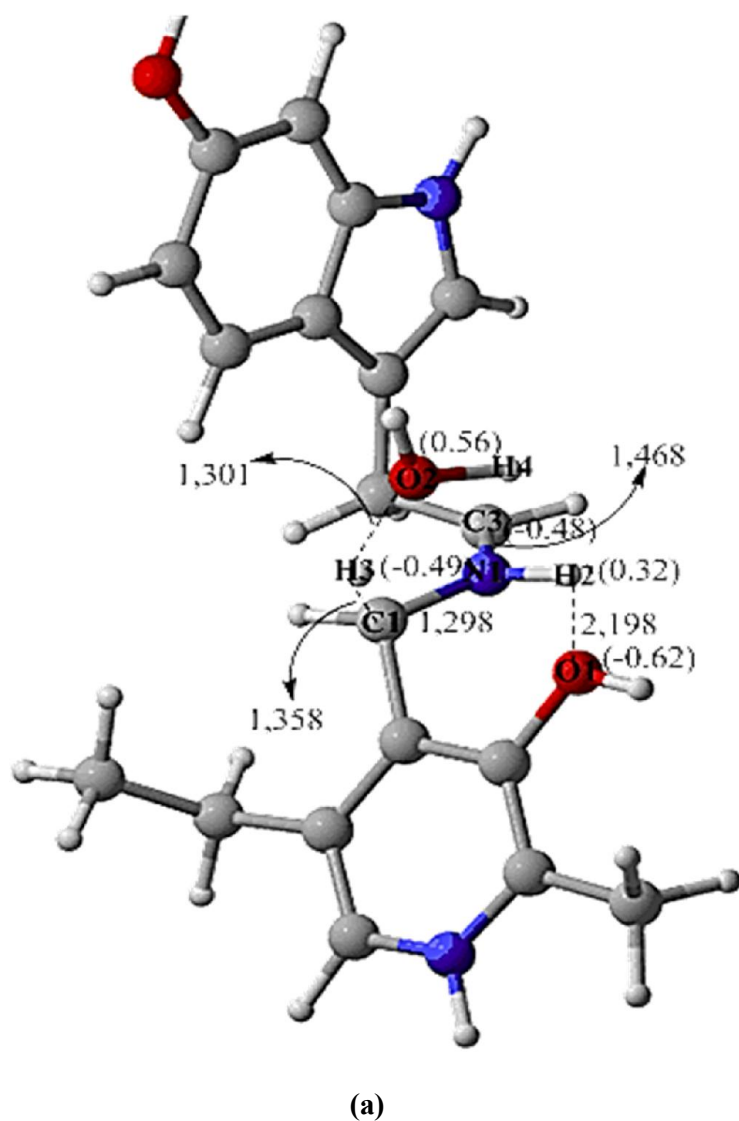


**Figure 3.13 :** Three dimensional geometries of formation of ketimine (structure 5\_s).  
a) Transition state (TS45\_s) with water assistance.



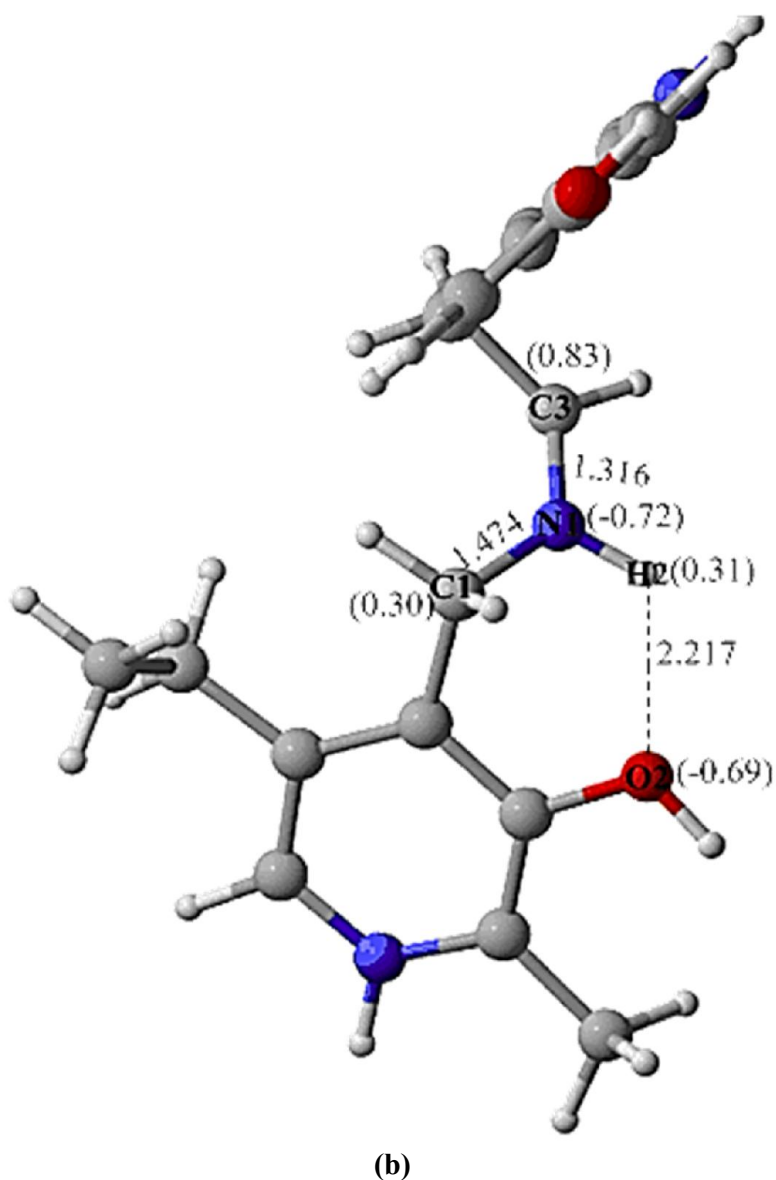


**Figure 3.13 (continued):** Three dimensional geometries of formation of ketimine (structure 5\_s). b) Geometry optimization result from forward IRC calculation. (structure 5\_s, ketimine).

### 3.5 Solvent Effect

The effect of the solvent on modeled mechanisms is studied with IEFPCM method. Only one type of solvent environment is chosen; water ( $\epsilon=78.39$ ). It was found that almost all the barriers are fall off while relative free energies that define the potential surface increased (Figure 3.15, Figure 3.16). The first step in external aldimine formation mechanism is the formation of substrate – PLP complex and proton transfer.

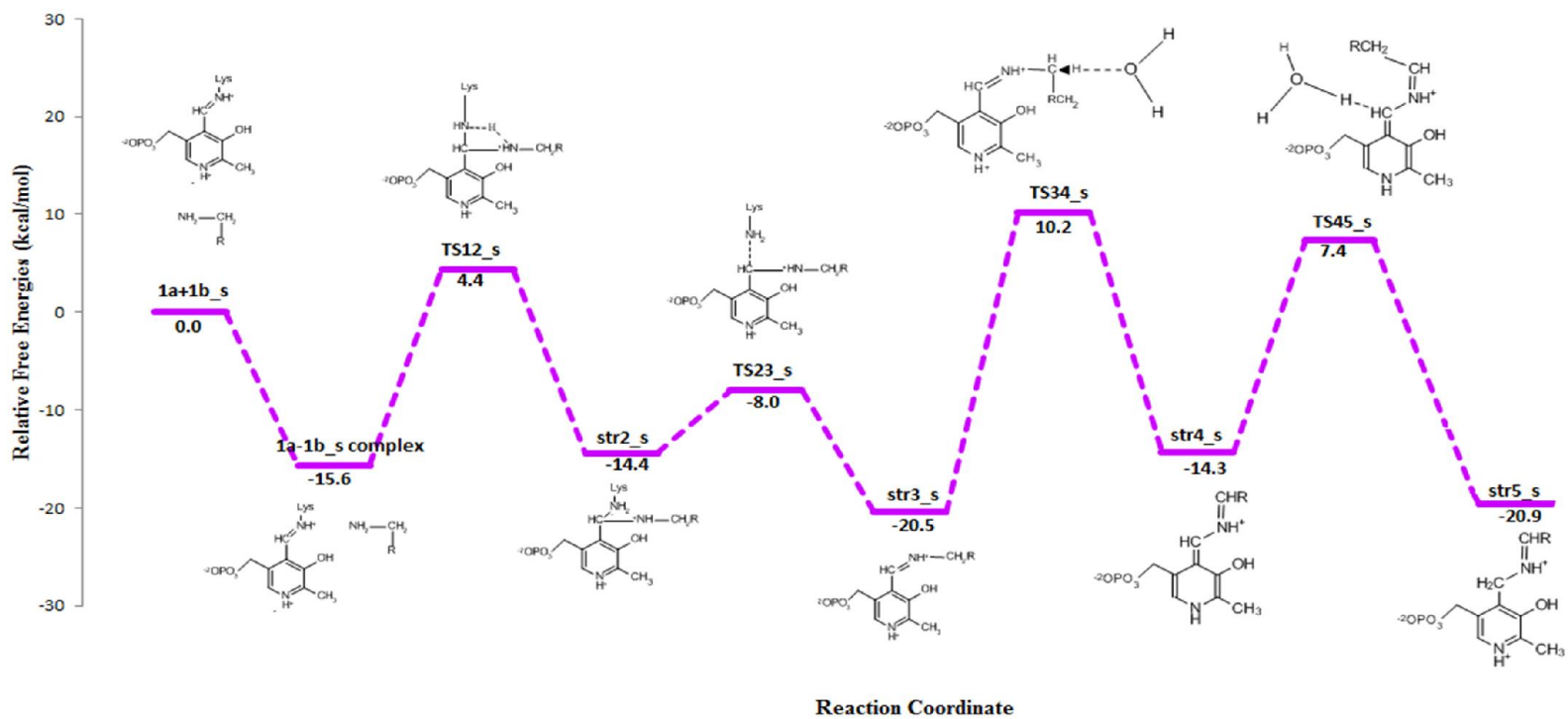


Figure 3.14 : Energy profile for 5-HT - DDC mechanism in gas phase. Relative free energies are given as kcal/mol

The methylamine – PLP – substrate complex has a relative energy as -16.6 kcal/mol for D-TrpMe and -15.6 kcal/mol for 5-HT in the gas phase while it increases to -3.3 kcal/mol and -6.2 kcal/mol respectively in water solvent. Moreover the relative energy for transition state structures TS12 is increased to 19.8 kcal/mol and TS12\_s is increased to 17.1 kcal/mol in the water from -16.6 kcal/mol and 15.6 kcal/mol respectively. The required energy barrier for this step is increased to 23.1 kcal/mol for D-TrpMe and 23.3 kcal/mol for 5-HT in the water solvent environment. Thus, it could be said that the increases in the energy barrier are almost same.

The step where the methylamine-Lys303 is removed from methylamine-PLP-serotonin complex (TS23\_s) has an energy barrier of 6.4 kcal/mol in gas phase. The energy barrier increases significantly to the 25.0 kcal/mol.

TS34 and TS34\_s where the proton transfer achieved by water assistance has an energy barrier of 30.4 kcal/mol and 30.7 kcal/mol respectively in the gas phase. The energy increase also seen in this step where the barriers increased to 38.3 kcal/mol and 33.0 kcal/mol respectively.

The last step (TS45, TS45\_s) is the proton transfer from hydronium to the quinonoid structure (str4, str4\_s) to form ketimine structure(str5, str5\_s). The required energy for this step is 21.7 kcal/mol for both transition state structures in the gas phase. When the calculations are performed in water, the energy barrier decreases to 6.4 kcal/mol for TS45 and 3.3 kcal/mol for TS45\_s.

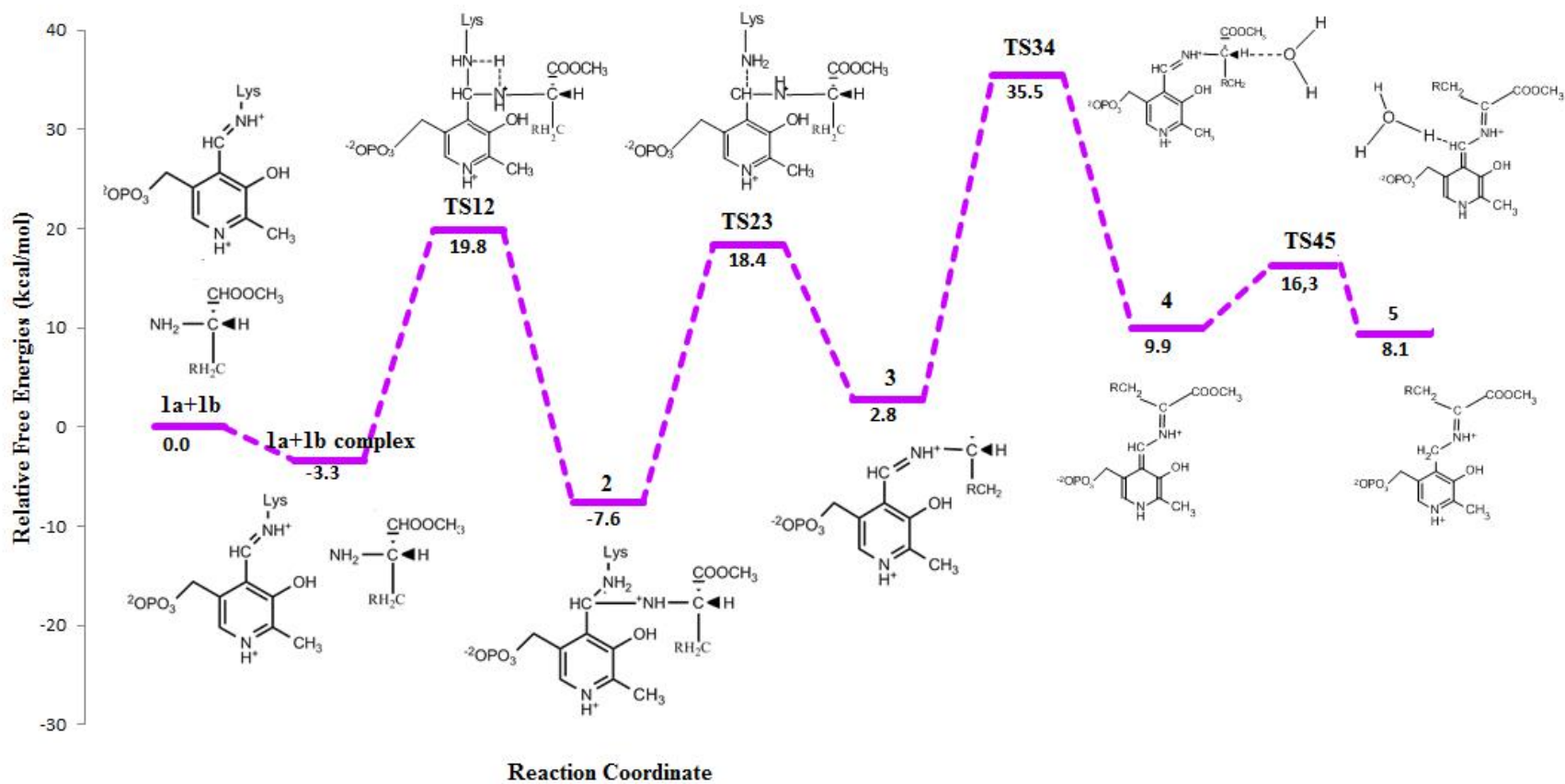


**Figure 3.15** : Energy profile for D-TrpME - DDC mechanism in solvent phase. Relative free energies are given as kcal/mol

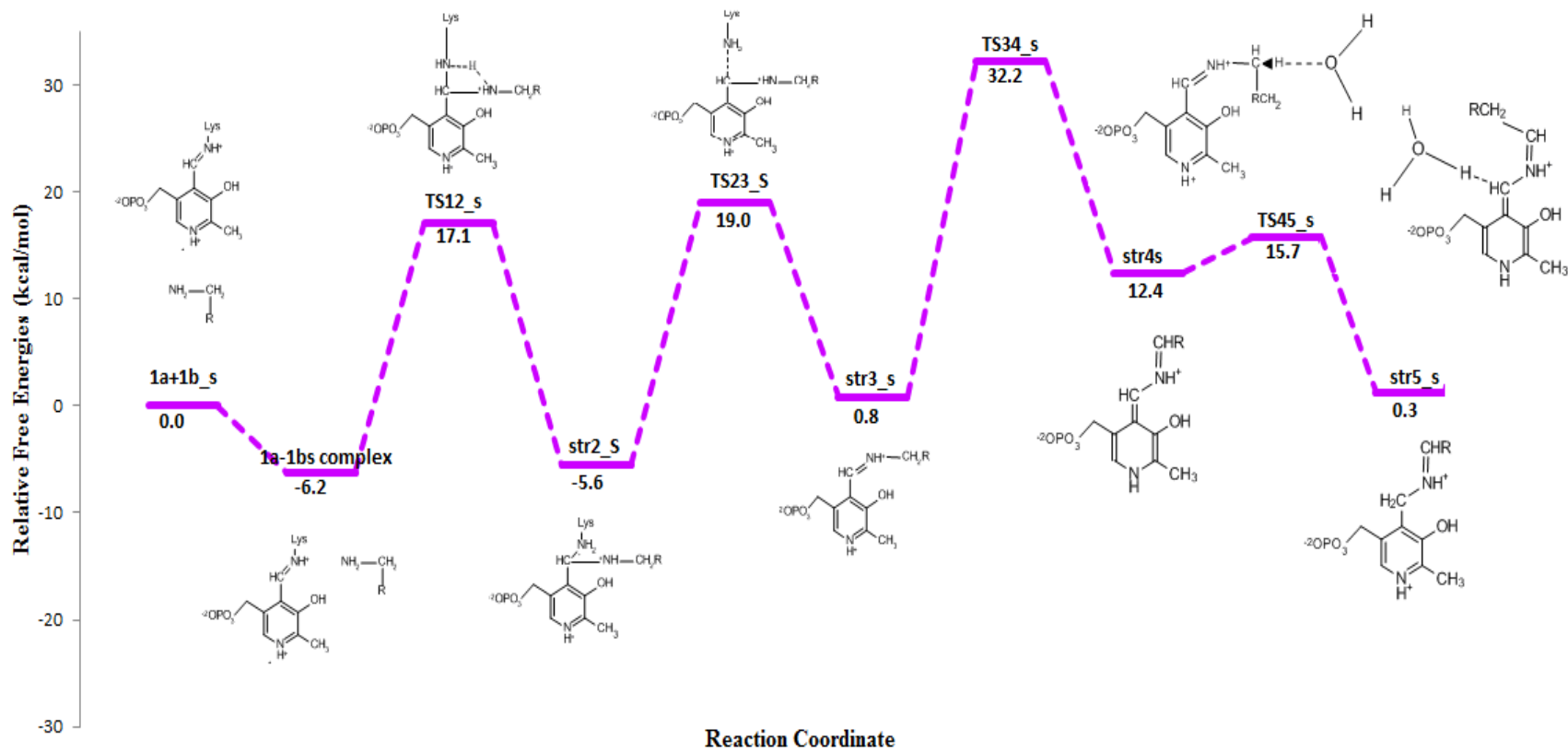


**Figure 3.16** : Energy profile for 5-HT- DDC mechanism in solvent phase. Relative free energies are given as kcal/mol



#### 4. CONCLUSION

In this thesis, a DFT study is carried out on the side reactions of DDC which lowers the activity of the enzyme. The half-transamination reaction is one of the side reactions of DDC studied computationally in the presence of two different substrates. The structural differences between D-Trptophan Methyl Ester and 5-Hydroxytryptophan result in competitive inactivation mechanism. The relative population of the products obtained from these two competitive inactivations are found to be  $K_{5-HT} / K_{D-TrpMe} = 9$  in harmony with the experimental findings.

The whole reaction path is found to be endergonic for D-trptophan methyl ester where in the presence of 5-Hydroxytryptophan, the reaction turns out to be neither exergonic nor endergonic. The probability of the formation of the reverse reaction is higher in the the case of D-TrpMe. This finding supports the superiority of the 5-HT relative to the D-TrpMe. In other words, the half transamination reaction can be categorized as thermodynamically controlled reaction.

Although the experimental results indicate that the step where the formation of quinonoid is achieved is not the rate determining step, computational results does not confirm this result. It should be noted that the experimental studies carried out for the oxidative deamination mechanism. The rate determining step is found to be the quinonoid formation with 35.5 kcal/mol and 32.2 kcal/mol relative free energies for D-TrpMe and 5-HT respectively. Our study is based on the computaitonal study on the side reactions. The difference can be rationalized based on the content of the studies.

Structure TS23, which is the last step of the formation of external aldimine, can not be obtained in gas phase calculations in the presence of carboxyl group on  $\alpha$ -Carbon (D-TrpMe). In order to obtain a transition state goemetry, carboxyl gorup is replaced by methyl group. The observed relative free energy value and free energy barrier for the methylated substituted structure is higher than expected. The gas phase calculation with the 5-HT substrate showed that the free energy barrier is around 6.5 kcal/mol having a relative free energy value of -8.0 kcal/mol. It is not possible to

propose a reliable barrier by using this approach. Transition state structure for charged species cannot be located in gas phase calculations. In addition results obtained from solvent phase calculations are more compatible to the experimental results. Therefore charged species must be studied in the solvent environment.

The results enable us to have an idea about one of the side reactions of DDC. However, there exists another side reaction which can contain a radical in the pathway. For a better explanation of the competitive reactions, one must also study that pathway. It should be also noted that a QM/MM study will be carried out for this reaction in order to identify the specificity of amino acid residues surrounding the active site.



## REFERENCES

- [1] **Bertoldi M, Cellini B, Maras B, Voltattorni CB.,** (2005). A quinonoid is an intermediate of oxidative deamination reaction catalyzed by Dopa decarboxylase, *FEBS Letter*, 26, 579, 5175-80.
- [2] **Bertoldi M. Moore P. S., Maras B., Dominici P., Voltattorni CB.,** (1996). Mechanism-based inactivation of dopa decarboxylase by serotonin *Journal of Biological Chemistry*, 271, 39, 23954-59.
- [3] **Alberts, B., Bray, D., Hopkin, K., Johnson, A., Lewis, J., Raff, M., Roberts, K., Walter, P.,** (2004). *Essential Cell Biology Second Edition*, Garland Science, Taylor and Francis Group, New York, USA, pp. 92, 93
- [4] **Silverman, R. B.,** (2002). *The Organic Chemistry of Enzyme-Catalyzed Reactions*, Academic Press, London, UK, pp. 2, 4, 6
- [5] **Lodish, H., Berk, A., Matsudaria, P., Kaiser, C. A., Krieger, C. A., Scott, M. P., Zipursky, S. Lawrance, Darnell, J.,** (2004). *Molecular Cell Biology Fifth Edition*, W. H. Freeman and Company, New York, pp. 73,74,75
- [6] **Nelson, D. L., Cox, M. M.,** (2000). *Lehninger Principles of Biochemistry*, W. H. Freeman & Co., New York, pp. 244, 245
- [7] **Gramatikova, S., Mouratou, B., Stetefeld, J., Mehta, P. K., Christen, P.,** (2002). Pyridoxal-5'-phosphate-dependent catalytic antibodies, *Journal of Immunological Methods*, 269, 99–110
- [8] **Ondrechen, M. J. , Briggs, J. M. , McCammon, J. A. ,** (2001). A model for enzyme-substrate interaction in alanine racemase, *Journal of American Chemical Society*, 123, 2830-2834
- [9] **Snell, E. E., in Dolphin, D., Poulson, R., Avramovic, O. (Eds.),** (1986). Vitamin B6 Pyridoxal Phosphate, *Chemical, Biochemical and Medical Aspects, Part A*, Wiley-Interscience, New York, USA, pp. 1 – 12
- [10] **Salva, S., Donoso, J., Frau, J., Munoz, F.,** (2002). Theoretical studies on Schiff base formation of vitamin b6 analogues, *Journal of Molecular Structure (Theochem)*, 577, 229-238
- [11] **Casasnovas, R., Salva, A., Frau, J., Donoso, J., Munoz, F.,** (2009). Theoretical study on the distribution of atomic charges in the Schiff bases of 3-hydroxypyridine-4-aldehyde and alanine. The effect of the protonation state of the pyridine and imine nitrogen atoms, *Chemical Physics*, 355, 149-156
- [12] **Salva, A., Donoso, J., Frau, J., Munoz, F.,** (2002). Theoretical studies on transimination of vitamin B6 analogs, *International Journal of Quantum Chemistry*, 89, 48-56

- [13] **Rando, R. R., Bangerter, F. W.,** (1977). Reaction of neurotoxin gabaculine with pyridoxal-phosphate, *Journal of the American Chemical Society*, 99, 15, 5141-5145
- [14] **Silverman, R. B., George, C.,** (1988). Inactivation of gamma-aminobutyric acid aminotransferase by (z)-4-amino-2-fluorobut-2-enoic acid, *Biochemistry*, 27, 3285-3289
- [15] **Fu, M., Silverman, R. B.,** (1999). Isolation and characterization of the product of inactivation of gamma-aminobutyric acid aminotransferase by gabaculine, *Biorganic & Medicinal Chemistry*, 7, 1581-1590
- [16] **Wang, Z., Yuan, H., Nikolic, D., Van Breemen, R. B. and Silverman, R. B.,** (2006). (+/-)-(1S, 2R, 5S)-5-amino-2-fluorocyclohex-3-enecarboxylic acid. A potent GABA aminotransferase inactivator that irreversibly inhibits via an elimination-aromatization pathway, *Biochemistry*, 45, 14513-14522.
- [17] **Ichinose H., Kurosawa Y., Titani K., Fujita K. and Nagatsu T.,** (1989). Isolation and characterization of a cDNA clone encoding human aromatic L-amino-acid decarboxylase, *Biochem. Biophys. Res. Commun.* 164, 1024-1030.
- [18] **Burkhard P., Dominici P., Borri-Voltattorni C., Jansonius J. N. and Malashkevich V. N.** (2001). Structural insight into Parkinson's disease treatment from drug-inhibited DOPA decarboxylase, *Nat. Struct. Biol.* 8, 963-967.
- [19] **Ishii S., Mizuguchi H., Nishino J., Hayashi H. and Kagamiyama H.,** (1996). Functionally important residues of aromatic L-amino acid decarboxylase probed by sequence alignment and site-directed mutagenesis, *J. Biochem. (Tokyo)*. 120, 369-376. [2]
- [20] **Bertoldi M. and Voltattorni C. B.,** (2009). Multiple roles of the active site lysine of Dopa decarboxylase, *Arch. Biochem. Biophys.* 488, 130-139.
- [21] **Dunathan H. C.,** (1966). Conformation and reaction specificity in pyridoxal phosphate enzymes, *Proc. Natl. Acad. Sci. U. S. A.* 55, 712-716.
- [22] **Bertoldi M., Castellani S. and Voltattorni C. B.,** (2001). Mutation of residues in the coenzyme binding pocket of Dopa decarboxylase - Effects on catalytic properties, *Eur. J. Biochem.* 268, 2975-2981.
- [23] **Ishii S., Hayashi H., Okamoto A. and Kagamiyama H.,** (1998). Aromatic L-amino acid decarboxylase: Conformational change in the flexible region around Arg334 is required during the transaldimination process, *Protein Sci.* 7, 1802-1810.
- [24] **Lucki I.,** (1998). The spectrum of behaviors influenced by serotonin. *Biol. Psychiatry* 44, 151-162.
- [25] **Koella W. P., Feldstein A. and Czicman J. S.,** (1968). The effect of parachlorophenylalanine on the sleep of cats, *Clin. Neurophysiol.* 25, 481-490.

- [26] **Breisch S. T., Zemlan F. P. and Hoebel B. G.**, (1976). Hyperphagia and obesity following serotonin depletion by intraventricular parachlorophenylalanine *Science* 192, 382-385.
- [27] **Simansky K. J. and Vaidya A. H.**, (1990). Behavioral mechanisms for the anorectic action of the serotonin (5-HT) uptake inhibitor sertraline in rats - comparison with directly acting 5-HT agonists, *Brain Res. Bull.* 25, 953-960. [2]
- [28] **Cools R., Calder A. J., Lawrence A. D., Clark L., Bullmore E. and Robbins T. W.**, (2005). Individual differences in threat sensitivity predict serotonergic modulation of amygdala response to fearful faces, *Psychopharmacology* (Berl). 180, 670-679.
- [29] **Cools R., Roberts A. C. and Robbins T. W.**, (2008). Serotonergic regulation of emotional and behavioural control processes, *Trends Cogn. Sci.* 12, 31-40.
- [30] **Yamada J., Sugimoto Y., Wakita H. and Horisaka K.**, (1988). The involvement of serotonergic and dopaminergic systems in hypothermia induced in mice by intracerebroventricular injection of serotonin *Jpn. J. Pharmacol.* 48, 145-148.
- [31] **Mink J. W. and Thach W. T.**, (1993). Combining versus gating motor programs - differential roles for cerebellum and basal ganglia, *Curr. Opin. Neurobiol.* 3, 950-957.
- [32] **Di Chiara G., et al.** (2004). Dopamine and drug addiction: the nucleus accumbens shell connection, *Neuropharmacology* 154, 173-211. Springer-Verlag, Berlin.
- [33] **Beninger R. J. and Hahn B. L.**, (1983). Pimozide blocks establishment but not expression of amphetamine-produced environment-specific conditioning, *Science* 220, 1304-1306.
- [34] **Hyland K., Surtees R. A. H., Rodeck C. and Clayton P. T.**, (1992). Aromatic l-amino-acid decarboxylase deficiency - clinical-features, diagnosis, and treatment of a new inborn error of neurotransmitter amine synthesis, *Neurology* 42, 1980-1988
- [35] **Swoboda K. J., Saul J. P., McKenna C. E., Speller N. B. and Hyland K.**, (2003). Aromatic L-amino acid decarboxylase deficiency - Overview of clinical features and outcomes, *Ann. Neurol.* 54, S49-S55.
- [36] **Robertson D., Haile V., Perry S. E., Robertson R. M., Phillips J. A. and Biaggioni I.**, (1991). Dopamine Beta-Hydroxylase Deficiency - A Genetic Disorder Of Cardiovascular Regulation, *Hypertension* 18, 1-8.
- [37] **Bertoldi M. and Voltattorni C. B.**, (2000). Reaction of dopa decarboxylase with L-aromatic amino acids under aerobic and anaerobic conditions, *Biochem. J.* 352, 533-538.
- [38] **Bertoldi M., Castellani S. and Voltattorni C. B.**, (2001). Mutation of residues in the coenzyme binding pocket of Dopa decarboxylase - Effects on catalytic properties, *Eur. J. Biochem.* 268, 2975-2981.

- [39] **Bertoldi M., Moore P. S., Maras B., Dominici P. and Voltattorni C. B.**, (1996). Mechanism-based inactivation of dopa decarboxylase by serotonin, *J. Biol. Chem.* 271,23954-23959.
- [40] **Bertoldi M, Cellini B, Maras B, Voltattorni CB.**, (2005). A quinonoid is an intermediate of oxidative deamination reaction catalyzed by Dopa decarboxylase, *Febs Letter*, 26;579(23):5175-80.
- [41] **Fitts, D. D.**, (1999), *Principles of Quantum Mechanics as Applied to Chemistry and Chemical Physics*, Cambridge University Press, New York, USA, p. 46
- [42] **Atkins, P., Friedman, R. S.**, (2005), *Molecular quantum mechanics 4ed*, Oxford University Press, USA , pp. 24, 249, 233
- [43] **Young, D. C.**, (2001), *Computational Chemistry: A Practical Guide for Applying Techniques to Real-World Problems*, John Wiley & Sons Inc., ISBN: 0-471-33368-9, pp. 42, 81-82, 100-101, 159-160, 173-174, 179, 369, 364, 79, 80, 206-207, 389-390, 100-101, 513-514, 520, 531-533, 521, 529 [4]
- [44] **Jensen, F.**, (1999), *Introduction to Computational Chemistry*, John Wiley & Sons Ltd., Chischester, England, pp. 150-151, 81-82, 182, 187-188, 392-393, 395, 230-231, 229 [4]
- [45] **Boys, S. F.**, (1950), Electronic Wave Functions. I. A General Method of Calculation for the Stationary States of Any Molecular System, *Proc. R. Soc. (London) A*, 200, 542
- [46] **Hinchliffer, A.**, (2003), *Molecular Modelling for Beginners*, John Wiley and Sons Ltd., Chichester, England, p. 325
- [47] **Stewart, J. J. P.**, (1989). Optimization of parameters for semiempirical methods, *J. Comput. Chem.*, 10, 209, 221
- [48] **Dreizler, R. M., Gross, E. K. U.**, (1990), *DFT - An Approach to the Quantum Many-Body Problem* , Springer – Verlag Berlin Heidelberg, Germany, pp. 66 – 68
- [49] **Eschrig, H.**, (1996), *The Fundamentals of DFT*, B. G. Teubner Verlagsgesellschaft Leipzig, Germany, p. 176
- [50] **von Rague Schlenyer, P.**, (1998), *Encyclopedia of Computational Chemistry*, Vol 1 A-D, John Wiley & Sons Ltd., Chichester, UK
- a. **Hu, C.-H. and Chong, D. P.**, *Density Functional Applications*, p. 664
  - b. **Gill, P. M. W.**, *Densit Functional Theory (DFT), Hartree-Fock (HF), and Self-Consistent Field*, 683
  - c. **Istvan Kolossvary, Wayne C. Guida**, *Conformational Analysis: 1*, pp. 513-520
  - d. **Ernest L. Eliel**, *Conformational Analysis: 3*, pp. 531-533
  - e. **Sandor Vajda**, *Conformational Analysis: 2*, pp. 521-529
- [51] **Hinchliffe, A.**, (2000), *Modelling molecular structures 2ed*, John Wiley & Sons Ltd., Chichester, England, pp. 224-225

- [52] **Koch, W., Holthausen, M. C.,** (2001), *A Chemists Guide to DFT 2ed*, Wiley-VCH Verlag GmbH, Weinheim, Federal Republic of Germany, p. 71
- [53] **Becke, D.,** (1993), *Physical Rev.* A140, pp. 1133-1138
- [54] **Stephens, P. J., Devlin, F. J., Chablowski, C. F. and Frisch, M. J.,** (1994), *Ab initio* calculation of vibrational absorption and circular dichroism spectra using density functional force fields, *J. Phys. Chem.*, 98, 11623
- [55] **Barton, D. H. R.,** (1950), *Experientia*, 6, 316-329, reprinted in *Top. Stereochem*, 1971, 6, 1-10
- [56] **Spartan '04**, Wavefunction Inc., 18401 Von Karman Ave., Suite 370, Irvine, CA 92612
- [57] **Gaussian 09**, Revision A.1, M. J. Frisch, G. W. Trucks, H. B. Schlegel, G. E. Scuseria, M. A. Robb, J. R. Cheeseman, G. Scalmani, V. Barone, B. Mennucci, G. A. Petersson, H. Nakatsuji, M. Caricato, X. Li, H. P. Hratchian, A. F. Izmaylov, J. Bloino, G. Zheng, J. L. Sonnenberg, M. Hada, M. Ehara, K. Toyota, R. Fukuda, J. Hasegawa, M. Ishida, T. Nakajima, Y. Honda, O. Kitao, H. Nakai, T. Vreven, J. A. Montgomery, Jr., J. E. Peralta, F. Ogliaro, M. Bearpark, J. J. Heyd, E. Brothers, K. N. Kudin, V. N. Staroverov, R. Kobayashi, J. Normand, K. Raghavachari, A. Rendell, J. C. Burant, S. S. Iyengar, J. Tomasi, M. Cossi, N. Rega, J. M. Millam, M. Klene, J. E. Knox, J. B. Cross, V. Bakken, C. Adamo, J. Jaramillo, R. Gomperts, R. E. Stratmann, O. Yazyev, A. J. Austin, R. Cammi, C. Pomelli, J. W. Ochterski, R. L. Martin, K. Morokuma, V. G. Zakrzewski, G. A. Voth, P. Salvador, J. J. Dannenberg, S. Dapprich, A. D. Daniels, Ö. Farkas, J. B. Foresman, J. V. Ortiz, J. Cioslowski, and D. J. Fox, Gaussian, Inc., Wallingford CT, 2009.
- [58] **Liao, R., Ding, W., Yu, J., Fang, W., Liu, R.,** (2008). Theoretical studies on pyridoxal 5'-phosphate-dependent transamination of alpha-amino acids, *J. Comput. Chem.*, 29, 1919
- [59] **A.T. Durak, H. Gökcan, F. A. S. Konuklar;** (2011). Theoretical studies on the inactivation mechanism of gamma-aminobutyric acid aminotransferase, *Organic and Biomolecular Chemistry*, Vol.9, 5162-5171.
- [60] **Gokcan, Hatice; Konuklar, F. Aylin Sungur,** (2012). Theoretical Study on HF Elimination and Aromatization Mechanisms: A Case of Pyridoxal 5' Phosphate-Dependent Enzyme, *Journal Of Organic Chemistry*, Vol.77, 5533-5543.



## **APPENDICES**

### **APPENDIX A: Energies**

**APPENDIX A****Table A.1** Gas Phase Gibbs Free Energies for D-TrpMe

	Gas phase free energy (Hartree)	Gas phase relative free energy (Hartree)	Gas phase relative free energy (kcal/mol)
1a	-574.676263		
1b	-725.519208		
1a+1b	-1814.829191	0.000000	0.00
TS12_rev	-1814.855628	-0.026437	-16.59
TS12	-1814.823680	0.005511	3.46
Str2	-1814.864189	-0.034998	-21.96
TS23			
Str3	-1814.861902	-0.032711	-20.53
TS34	-1814.813414	0.015777	9.90
Str4	-1814.853922	-0.024731	-15.52
TS45	-1814.819310	0.009881	6.20
Str5	-1814.858261	-0.029070	-18.24

**Table A.2** Gas Phase Gibbs Free Energies For Serotonin

	Gas phase free energy (Hartree)	Gas phase relative free energy (Hartree)	Gas phase relative free energy (kcal/mol)
1a	-575.148858		
1b	-725.734002		
1a+1b	-1815.21988	0	0
TS12_rev	-1815.24474	-0.02486016	-15.6
TS12	-1815.21287	0.00701184	4.4
Str2	-1815.24283	-0.02294784	-14.4
TS23	-1815.23263	-0.0127488	-8
Str3	-1815.2526	-0.03271661	-20.5
TS34	-1815.20363	0.016254721	10.2
Str4	-1815.24267	-0.02278848	-14.3
TS45	-1815.20809	0.011792641	7.4
Str5	-1815.25319	-0.03330624	-20.9



**Table A.3** PCM Energies (solvent=water) for D-TrpMe

	PCM Energy (Hartree)	Relative PCM Energy (Hartree)	PCM Energy (kcal/mol)
1a	-575.148858		
1b	-725.734002		
1a+1b	-1815.21988	0	0
TS12_rev	-1815.22514	-0.00525888	-3.3
TS12	-1815.18833	0.031553282	19.8
Str2	-1815.23199	-0.01211136	-7.6
TS23	-1815.19056	0.029322242	18.4
Str3	-1815.21542	0.00446208	2.8
TS34	-1815.16331	0.056572804	35.5
Str4	-1815.20411	0.015776641	9.9
TS45	-1815.19391	0.025975682	16.3
Str5	-1815.20698	0.012908161	8.1

**Table A.4** PCM Energies (solvent=water) for Serotonin

	PCM Energy (Hartree)	Relative PCM Energy (Hartree)	PCM Energy (kcal/mol)
1a	-575.148858		
1b	-573.07117		
1a+1b	-1224.66231	0	0
TS12_rev	-1224.67219	-0.00988032	-6.2
TS12	-1224.63506	0.027250562	17.1
Str2	-1224.67123	-0.00892416	-5.6
TS23	-1224.63203	0.030278402	19
Str3	-1224.66103	0.00127488	0.8
TS34	-1224.611	0.051313923	32.2
Str4	-1224.64255	0.019760641	12.4
TS45	-1224.63729	0.025019522	15.7
Str5	-1224.66183	0.00047808	0.3



## **CIRRICULUM VITAE**

**Name Surname** : Erdem ÇİÇEK  
**Place of birth** : ANKARA  
**Date of birth** : 25.07.1984  
**Adres** : ITU Graduate School Of Science, Engineering and  
Technology  
**E-Mail** : ciceke@itu.edu.tr  
**B.Sc.** : ITU Molecular Biology and Genetics (2003 – 2008)